Presented at 8th Annual Missile
and Space Technology Institute
Univ. of Connecticut, Aug. 4-5, 1965

NON-CHEMICAL PROPULSION

by John C. Evvard

Lewis Research Center
National Aeronautics and Space Administration
Cleveland, Ohio

I. INTRODUCTORY PRINCIPLES

First, consider a rocket in gravity free space. To obtain thrust, a

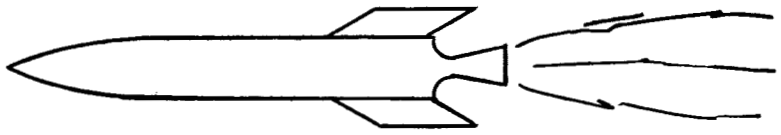

propellant must be ejected from the rocket. The reaction force on the rocket is calculated from Newton's laws as

$$F = \frac{dmu}{dt} = u\,\frac{dm}{dt} \qquad (1)$$

where u is the constant ejection velocity of the propellant and dm/dt is the rate of propellant consumption. Now, let us assume that the propellant is ejected as a gas which has a total energy per unit weight of C_pT, where C_p is the specific heat at constant pressure per unit weight and T represents the temperature of the gas before it passes through the exhaust nozzle. Now, as the gas passes through its exhaust nozzle, this internal energy will be converted to velocity. Conservation of energy at any point along the way then says that the thermal energy of the gaseous propellant plus the kinetic energy is equal to the original energy.

$$C_pt + \frac{1}{2}u^2 = C_pT, \text{ a constant} \qquad (2)$$

Thus, as the propellant of a rocket expands through the exhaust nozzle, the kinetic energy, $\frac{1}{2}u^2$, increases at the expense of the thermal energy term, C_pt. The maximum jet velocity for complete expansion is therefore

$$u = \sqrt{2C_pT} = \sqrt{\frac{2\gamma RT}{(\gamma - 1)W}} \qquad (3)$$

where γ is the ratio of specific heats at constant pressure and constant volume, W is the molecular weight, and R is the universal gas constant. The third member of equation (3) results from application of the thermodynamic relations

$$C_p - Cv = \frac{R}{W} \quad \text{and} \quad \frac{C_p}{Cv} = \gamma$$

[redacted]s (3) and (1) we see that the thrust of a fully ex-

$$F = \frac{dm}{dt}\sqrt{\frac{2\gamma RT}{(\gamma - 1)W}}$$

[redacted]ance is achieved with low molecular weight propellants at the highest temperature. Let me define the term "specific impulse" as the force in weight units (F/g) exerted when one weight unit per second of propellant flows. Hence:

[redacted]

$$I = \frac{F/g}{dm/dt} = \frac{u}{g} = \frac{1}{g}\sqrt{\frac{2\gamma RT}{(\gamma - 1)W}} \qquad (4)$$

Jet velocity and specific impulse are essentially the same except for the gravitational constant "g."

From Newton's laws, the acceleration of the rocket in space is thus

$$F = \frac{m\ dv}{dt} = Ig\ \frac{dm}{dt} \qquad (5)$$

Integration gives:

$$\Delta v = Ig\ \ln \frac{m\ (\text{initial})}{m\ (\text{final})} \qquad (6)$$

Thus, the velocity increase of the rocket case and payload is proportional to the specific impulse and to the ln of the initial to final mass ratio for that stage. The velocity increment is independent of the size of the rocket in this relation.

A two-stage rocket will give twice the Δv of a one-stage rocket but the respective mass ratios are multiplied. For example, take rockets that have a mass fraction of 10/1 with a Δv of 10,000 feet per second per stage. The following table then pertains:

Number of stages	Δv	Mass fraction per stage	Overall mass fraction
1	10,000	10	10
2	20,000		100
3	30,000		1000

One might suppose from the above discussion that the highest jet speeds (i.e., the highest specific impulses) possible are always desired. This conclusion is generally true for the chemical rocket providing that other factors such as propellant density do not compromise the rocket propellant to structural weight fraction. It may not be true for advanced nuclear or electric rockets for which the energy source is independent of the propellant. From equation (1), the jet thrust increases as the jet speed. The jet power, on the other hand, increases as the square of the speed relative to the spacecraft. If the thermal energy of the jet is neglected,

$$P = \frac{1}{2}\dot{m}u^2 \qquad (7)$$

From equation (1), the jet power per poundal of thrust is:

$$\frac{P}{F} = \frac{u}{2} = \frac{Ig}{2} \qquad (8)$$

The propellant flow rate per poundal of thrust is:

$$\frac{\dot{m}}{F} = \frac{1}{u} = \frac{1}{Ig} \qquad (9)$$

Hence, the product

$$\left(\frac{\dot{m}}{F}\right)\left(\frac{P}{F}\right) = \frac{1}{2}, \text{ a constant} \qquad (10)$$

This relation is shown on slide 1. Thus, if only low grade energy sources are available, such as in the chemical rocket, large mass flow rates will be required. The vehicle weight at take-off will be principally propellant.

On the other hand, if high grade energy sources such as nuclear fission or fusion are available, then higher specific impulses (jet velocity) may be employed leading to lower fuel consumption rates. Under such circumstances, the power generation system weight may become as important or more important than the propellant weight. The trade-off between propellant weight and power plant weight gives a requirement for an optimum specific impulse which may vary along the flight trajectory.

The total propellant load is proportional to the product of the propellant consumption rate and the time period that the propellant is being used. For a given mission, we may thus represent the propellant load by the rectangular hyperbola. The shape and position of the hyperbola depends on the propulsion time, so that the curve moves up or down on the graph accordingly as the mission is more, or less challenging. The weight of the propellant plus power plant which we wish to minimize thus depends on the mission propulsion time as well as the powerplant specific weight. Clearly, the sum of propellant plus powerplant weight has a minimum, suggesting an optimum specific impulse at the point of intersection of the straight line and the rectangular hyperbola. If the mission times are increased, higher required specific impulses result. Lower specific powerplant weights also suggest higher specific impulses.

II. THE NUCLEAR ROCKET

We have seen the importance of specific impulse to the performance quality of rockets. The chemical rocket has a maximum specific impulse of perhaps less than 500 seconds. This limit results because the chemical

reaction required to achieve the high exhaust temperature also gives a gas with compensatingly high molecular weight. On the other hand, a nuclear reactor might be used to heat hydrogen as the propellant to maintain a low molecular weight. In this case, the maximum temperature of the gas is limited by the materials available for constructing the reactor. Utilizing equation (4), the specific impulse then calculates to be in the range from 750 to 1,000 depending upon various assumptions. With such impulses, the nuclear rocket offers perhaps a 5 fold reduction in interplanetary spacecraft weight over that of the chemical rocket.

A schematic drawing of a solid core heat transfer type nuclear rocket is shown in slide 2. The fission energy is liberated within solid materials of which the reactor core is composed. This heat is transferred to hydrogen as it passes through the axial heat transfer passages on the way toward the exhaust nozzle. The liquid hydrogen is pumped from the propellant tank through the nozzle walls and reflector for cooling purposes. The vaporized hydrogen then passes through the reactor and nozzle to produce thrust.

The heat of the reactor is, of course, derived from the fission of high atomic weight elements such as U_{235}. A neutron enters the uranium atom to cause fission into several fragments of lower atomic weight. Additional neutrons are also released to cause other uranium atoms to fission. The type of reactor design depends upon how these additional neutrons are conserved.

The neutrons are quite energetic when they are liberated from a fissioning atom. However, the probability of interaction with another uranium atom is increased if the neutrons are slowed down. This can be accomplished by use of a moderating material in which the neutrons are randomized to thermal velocities.

A homogeneous thermal reactor is one in which the fissionable material is intimately mixed with the neutron moderating material as shown in slide 3(a). The heat deposited in this moderator by fission is removed by passage of hydrogen through an array of coolant tubes running from one end of the reactor to the other. In addition to slowing down the neutrons, the moderator must serve as a high temperature heat exchanger. Graphite and beryllium oxide are the only two materials that can reasonably serve this dual function. Graphite has the poorer moderating properties of the two, and therefore its use leads to larger core dimensions and weight. On the other hand, beryllium oxide is limited to operating temperatures of at least 1000° F less than that of the graphite. Since specific impulse is so important, graphite is really the only contender in this homogeneous type reactor.

Unfortunately, hydrogen attacks hot graphite forming acetylene and other gaseous compounds. Hence, the use of graphite requires a protective coating on the heat transfer passages to prevent chemical reaction and corrosion in the hot hydrogen atmosphere. The Los Alamos Laboratory has spent a great deal of effort developing coatings that might be used to protect the graphite [redacted]

The first nuclear rocket reactors are graphite moderated. They were designed by the Los Alamos Laboratory and are undergoing tests at the Jackass Flats area of the Nevada Test Site located 90 miles northwest of Las Vegas. This is the KIWI program named after the flightless New Zealand bird. Thus far (July 1964), six KIWI reactor tests have been run at nuclear power. These were all research reactors and hence were subject to failure and the release of fission products to the atmosphere. Hence, the test area must include large exclusion distances as are shown on slide 4. In addition, an elaborate ground instrumentation program has been set up in each of the reactor test areas and around the perimeter of the site. Runs are permitted only under favorable wind and weather conditions. The Los Alamos Laboratory, the Public Health Services, the U.S. Weather Bureau, and the Reynolds Electric and Engineering Company cooperate to determine the generation of fission product activity, the amount that escapes from the reactor, how much is released to the atmosphere, and where it goes. This radioactivity release is, of course, near the surface. Also, the maximum creditable accident would produce no more than 1 percent of the fission products generated in a normal run. So these tests are surely safe as far as the public welfare is concerned.

While we are on the subject, you might ask about the possible contamination of the upper atmosphere through nuclear rocket flight. Prior to the resumption of testing by the Russians, the Earth's biospheric burden contained long-lived isotopes from some 90,000 kilotons of weapons testing, which decay at a rate of about 2 percent per year. If we were to operate reactors having a power output of 10,000 megawatts for five minutes of flight, and then disintegrate them so as to release all the fission products formed, we would have had to conduct 1000 such flights per year just to equal the decay rate of the biospheric burden. Nuclear rocket contamination of the upper atmosphere would thus be trivial.

Of more concern is the possibility that the reactor might enter the ocean intact. If this occurred, the water would serve as a moderator for the reactor leading to a nuclear excursion that could result in the release of much of the fission product inventory. The reactor could contain up to 50 curies of Strontium 90. The National Academy of Sciences indicates that one can release 25,000 curies of Strontium 90, or the biological equivalent in deep water exceeding 1000 fathoms (six feet per fathom) without creating an undue hazard. Beyond the continental shelf, such depths are matched or exceeded. You might be interested to know that if 50 curies of Strontium 90 are distributed in a sphere of water 500 meters in diameter, the water is drinkable.

The KIWI A series reactors were fed with gaseous hydrogen and the exhaust nozzle was cooled with liquid water. The reactors tested as part of the KIWI B program aimed at developing a basic core design that could be engineered for flight application. Power experiments were run using liquid hydrogen as coolant, with a regenerative, liquid hydrogen-cooled jet nozzle. These tests were to provide the preliminary design information for the NERVA reactor program.

An aerial view of Test 1, Site A is shown on slide 5. This stand has a capacity of about 3.0 million standard cubic feet of gaseous hydrogen and about 56,000 gallons of liquid hydrogen. Slide 5 shows the liquid storage vessels on the right. The building in the center houses instrumentation and the equipment to pump the hydrogen through the reactor which would be tested on the railroad siding just behind the concrete shield. The weather protection garage in the upper left hand corner is rolled out of the way during a test firing.

Figure 6 shows the KIWI B-1A reactor mounted in place ready for a firing. The exhaust products are discharged upward in these experiments contrary to the mode of flight operation. Following the firing, the reactor is transported along a remotely controlled railroad (slide 7) to the MAD building shown in slide 8. MAD stands for Maintenance Assembly and Disassembly. There the reactor is disassembled and examined behind shielded walls with unique remotely operated hot lab equipment.

Another larger test stand C is shown in slide 9. This stand has a gaseous hydrogen capacity of 4.5 million standard cubic feet and a liquid hydrogen capacity of 100,000 gallons. The spherical 50,000 gallon dewars had to be fabricated in place. The KIWI tests were initially run in test cell A but they have now been moved to test cell C. The objective of the KIWI program is to establish the research information on graphite reactors for rocket applications. The NERVA program is designed to develop the first nuclear rockets for flight applications as may be inferred from the name - Nuclear Engine for Rocket Vehicle Application. The NERVA contractor now uses test cell A for his reactor tests. The reactor was constructed at the Westinghouse Astronuclear Division plant in Pittsburgh and was transported to Jackass Flats by means of truck (slide 10) and railroad (slide 11).

A mock-up of the NERVA reactor is shown on slide 12. The exhaust nozzle is on the bottom. You may observe two vertical pipes. The one on the left carries liquid hydrogen from the pump down to regeneratively cool the exhaust nozzle. The one on the right carries hot hydrogen bleed gas from the reactor discharge plenum up to the turbine located just below the pump. You may also note several spools at the top of the reactor located around the periphery. These are part of the nuclear reactor control system. This system consists of a collection of cylindrical drums located around the periphery and running parallel to the reactor axis. Each drum contains moderating material on one side and neutron absorption material (poison) on the other side. Hence, the reactivity may either be enhanced or retarded by rotating the cylinders. Above the pump housing, you can see the conical shaped thrust structure. The propellant tank would lie above this fairing. The two spheres are gas bottles to feed the pneumatic actuators for the unit.

A schematic of the rocket system is pictured in slide 13. The reactor drum controls first bring the reactor from a subcritical condition to about 10 percent of full power. Some propellant flow is then initiated by tank pressure but the pump is not yet operating. This low hydrogen flow is then vaporized through the heat capacity of the nozzle and reactor to the exhaust and to the blue line leading to the turbine. This drives the pump leading

to greater propellant flow while the power level of the reactor is raised. Thus, the nuclear rocket is bootstrapped to power. The whole process is relatively long - being on the order of 10 to 30 seconds. The complete NERVA system will be evaluated at Jackass Flats at ETS-1 (Engine Test Stand 1). It will be fired vertically downward from a boiler plate type hydrogen tank. Altitude exhaust will be simulated by diffusing the flow downstream of the nozzle, bringing the pressure back up to atmospheric pressure at the discharge.

Important results have been obtained in the KIWI series, indicating that the method of reflector drum control is an effective one and that the reactor can be started in a controlled manner with liquid hydrogen. This was a worry, you see, because addition of liquid hydrogen to the core could serve as a moderator to increase the nuclear reactivity.

However, the power test run of November 30, 1962 on the KIWI-B4A reactor was far from trouble-free. This was the favored basic design for flight development. Severe vibrations were encountered early in the test run. Examination of the reactor indicated cracking in almost all of the fuel elements and damage to certain insulation components surrounding the core. At first, it was thought that the difficulty might have arisen through coupled instabilities in the two-phase liquid hydrogen, gaseous hydrogen system. Later, the difficulty was traced to quite a different cause.

The mechanical design of the reactor allowed a vibrational coupling with the pressure forces so that the reactor structure would breathe. High pressure hydrogen would leak down through the reactor structure to expand it. The expansion then spread the structure to relieve the gas pressure and reactivate the cycle.

Non-nuclear simulation tests have since been run replacing the fuel elements with unloaded graphite. These tests were run with nitrogen, helium, and hydrogen with pressure drops through the core similar to those that existed during a normal reactor startup. Vibrations were encountered similar to those of the November 1962 nuclear test and simple design modifications have been incorporated that eliminated the vibrations. These design modifications have been incorporated into both the KIWI and the NERVA reactor systems.

A KIWI reactor test occurred on May 14, 1964 to check out the design improvements. Unfortunately, there was a hydrogen leak in the piping leading to the reactor. Nevertheless, the run was continued for about 60 seconds before shutdown. As far as the reactor is concerned, this test was quite successful. The reactor was operated at full power without any visual signs of deterioration. There was no evidence of any debris being ejected from the nozzle, for example, as on previous tests. Other successful tests on several reactors including restarts have been conducted since then.

There are at least two other reactors that might be useful for nuclear propulsion. In the fast reactor shown on slide 3(b), no moderator is em-

ployed. Hence, the uranium content must be increased to compensate for the poorer neutron cross section statistics for the fast neutrons.

Fast reactors can be made very small and can use the best available fuel-bearing or fuel-containing materials. The largest drawback stems from the fact that nuclearwise fast reactors are less efficient than moderated systems and a great deal more fissionable material is required for criticality. This leads to more difficult materials problems, since the volume of fissionable materials must be approximately equal to the total volume of all other materials in the core. Unfortunately, since fissionable compounds are not very satisfactory as structural or heat transfer materials, they must be contained within a refractory material such as tungsten, molybdenum, or the carbide of zirconium, hafnium, or tantalum.

Development of fuel elements that contain 50 volume percent of fissionable material without penalizing high temperature performance is difficult. There are also difficult control problems associated with local thermal gradients during start-up. Nevertheless, the Argonne Laboratory is studying the feasibility of fast reactors with quite a bit of enthusiasm as a backup to the graphite reactor program.

At the Lewis Research Center, we have been more interested in a heterogeneous thermal reactor as a potential backup. In the heterogeneous arrangement (slide 3(c)), the fuel elements are separated from the moderator. Hence, the best materials for each can be employed. This type of reactor is not new. It received considerable attention by the General Electric Company in the ANP program in a reactor labeled HTRE 1. In that reactor, slide 14, the nichrome-contained fuel element was inserted into insulated aluminum tubes surrounded by water. The air to be heated passed over the nichrome fuel elements mounted inside the aluminum tubes. In the nuclear rocket application, tungsten would replace the nichrome in order to give higher gas temperatures.

The embodiment of this concept as a nuclear rocket is shown in slide 15. The hot fuel elements would be insulated from and contained in the multiplicity of aluminum tubes. The fuel elements would be cooled, of course, by the flowing hydrogen propellant. This array of tubes, along with the water moderator that surrounds them, constitutes the reactor. During full power operation, perhaps 7 to 8 percent of the reactor power would be deposited in the water. The water must therefore be cooled by the hydrogen. Hence, the hydrogen propellant from the pump first regeneratively cools the exhaust nozzle, then passes through this heat exchanger to cool the water. The heating of the propellant is completed in the reactor from whence it passes through the exhaust nozzle to space.

Slide 16 shows a sectioned view of a typical fuel element tube. The element itself might assume many different shapes such as parallel flat plates, honeycomb shapes, bundles of circular tubes, etc. I have chosen, for illustration purposes, this fuel element formed of five concentric cylinders of tungsten-clad UO_2 material. The fuel cylinders are supported and spaced by transverse support pins. The upstream pins (flow is from left to right in the slide) pass through and are fastened to a tungsten fuel support tube. This

fuel support tube runs the entire length of the reactor and provides a 1/8 inch gap between it and the water-cooled aluminum tube to decrease conduction heat transfer. This 1/8 inch gap might contain stagnant hydrogen at the reactor operating pressure. Radiation shields might also be inserted if the radiation heat load were greater than the neutron and gamma heating that might be deposited in the shield. These simple insulation techniques reduce the conduction heat losses from the fuel cylinders and the hot hydrogen to a fraction of 1 percent of the full reactor power compared to 6 or 7 percent heat load deposited in the water from neutron and gamma heating.

Slide 17 shows a photograph of a full-scale model. An aluminum pressure vessel is completely filled with water except for the aluminum tubes which contain the tungsten fuel elements and flowing hydrogen. The water to hydrogen heat exchanger is divided into six equally spaced segments, one of which is shown at the top. The hydrogen from the nozzle cooling passages enters the tubes of this heat exchanger where it removes the heat deposited in the water. The hydrogen then enters the reactor inlet plenum. From this region, the hot hydrogen is expanded through the nozzle (not shown) to produce thrust at a specific impulse of 800 to 900 seconds. The water moderator is circulated through the core and heat exchanger by means of a pump and inlet and outlet water plenum.

The capture cross section for neutrons in uranium is substantially increased by slowing the neutrons down to thermal velocities. That is the principal purpose for the water moderator in this reactor concept. The hydrogen in the water molecule thermalizes the neutrons through "equal mass" collision.

On the other hand, natural tungsten also exhibits strong resonance capture cross sections for thermalized neutrons as shown on slide 18. If the low energy neutrons were to be captured by the tungsten, they would no longer be available to continue the chain reaction. This capturing can largely be eliminated by using the tungsten 184 isotope rather than the natural material.

Nuclear physics calculations will give an estimate of reactivity improvement associated with the use of tungsten 184. Slide 19 shows a representative core region consisting of an array of fuel elements surrounded by water moderator regions. For ease of calculation, the equivalent cylindrical cell pictured in the center is employed to estimate the flux variation in the lattice cell.

The effect of enrichment of the tungsten 184 isotope as well as the effect of the water moderator thickness for this idealized geometry is estimated on slide 20. The cell multiplication factor K is simply the number of neutrons produced by fission per neutron absorbed in the cell. Since the cell multiplication factor is a measure of reactivity for an infinite number of these cells, the excess above unity must be used to supply the neutrons to be lost by leakage from a finite critical reactor size. The value of K reaches a peak at 1.18 for natural tungsten but for enriched tungsten, K

can be greater than 1.5. These peak values occur for water thickness between 0.5 and 1.0 inch. Thus, a reactor with fuel elements clad with natural tungsten would necessarily be very much larger than an enriched tungsten reactor, assuming the same fuel element uranium loading. Correspondingly, very much less uranium would be needed in the tungsten 184 reactor.

The separation cost for tungsten 184 is quite a bit less than the cost of uranium. In this sense, construction of the reactor from tungsten 184 appears to be an economy.

In our preliminary experiments, we have been able to manufacture sample fuel elements that satisfactorily contained uranium in hot tungsten-clad geometries. The problem of insulating the aluminum tubes from the hot gas stream appears to have a simple solution. There are no serious chemical reactions between the hydrogen and the tungsten. Tungsten 184 can be produced in sufficient quantity without hampering the current uranium purification program. We are currently evaluating a proposed heat exchanger to cool liquid water with liquid hydrogen. Preliminary data shows no serious problem. And we are building hot hydrogen facilities to evaluate the nozzle heat transfer problems as well as to evaluate the non-nuclear integrity of the fuel element in a flowing hot hydrogen reactor simulated gas stream. Thus we have a good start on the preliminary research necessary to establish this nuclear reactor concept.

It is apparent that the high temperature problems of this reactor concept are concentrated within individual isolated small fuel elements. The remainder of the reactor is made entirely of aluminum which is water-cooled at all points. This major structural component can be developed to a high degree of perfection without resorting to full scale nuclear testing. In fact, one of the beauties of this whole reactor concept is that it is highly susceptible to component evaluation and improvement without requiring a full scale test in the early stages of development.

I would like to conclude this discussion of the nuclear rocket with a few comments concerning their use. To begin with, anything nuclear has political repercussions. While nuclear engines could feasibly be safely used to boost space payloads into orbit, the probability is high that such flights would not initially be permitted. Hence, getting to orbit will be accomplished by chemical means.

The graphite nuclear rocket is heavy even without nuclear shielding. Hence, nuclear propulsion could not be justified for the smaller missions. An approximate number to remember is that the vehicle take-off weight from a 300-mile parking orbit must exceed 50,000 pounds to justify nuclear propulsion over high energy chemical rockets. Of course, a manned round trip expedition to Mars via nuclear propulsion would require more than a million pounds of spacecraft in earth orbit.

On slide 21, I have compared the performance of nuclear and chemical rockets. You can easily see that nuclear propulsion offers substantially higher Δv's or substantially higher payload weights than can be used with high energy chemical rockets. This particular comparison used relatively low power nuclear rockets compared to current thinking. However, the advantages of nuclear rockets in large sizes are even more obvious. For lunar missions, the use of nuclear rockets allows an increase of the payload by 30 to 60 percent of the launch vehicle weight as compared to the chemical rocket. For manned missions to Venus or Mars, the payload is increased by at least 100 percent and the mission time may be cut by a factor of two.

For manned nuclear flight, careful consideration of the radiation hazard is, of course, required. In the early phases of the mission, the large propellant load can serve admirably for shielding. The shielding requirements for the terminal phases need more study but, in general, the feeling persists that the reactor shielding requirements are modest. People are much more worried about giant solar flares, Van Allen belts, and cosmic rays in about that order.

III. THE SOLAR-HEATED HYDROGEN ROCKET

We have seen from equation (4) that the specific impulse of a rocket, utilizing hydrogen as the sole propellant, depends principally on the temperature to which hydrogen can be heated. In the nuclear heat transfer rocket, this limit is set by the properties of materials. Krafft Ehricke and others have proposed that solar energy replace the nuclear reactor. In this way, the nuclear radiation hazards are avoided as well as the shielding problems. However, a new set of problems must be faced including those of the collector and the requirement for precise orientation relative to the sun. Also, because the sunlight only has about 1.34 kilowatts of energy per square meter at Earth's distance, you can see that the required solar collector area could become very large. The nuclear rockets we discussed were on the order of thousands of megawatts. Hence, millions of square meters of solar collector area would be required. Also, the idea does not work in the shadow of a planet. I nevertheless wanted to call your attention to this idea.

IV. ELECTRIC PROPULSION

The electric rocket refers to a rocket system requiring electric energy to accelerate the exhaust jet. Electric rockets can, in general, give exhaust velocities greater than are achievable by chemical means. The acceleration of a singly charged positive ion through a potential drop of only one volt would correspond to a chemical rocket combustion temperature of $11{,}600^{\circ}$ K - and many thousands of volts of acceleration are feasible. Hence, electric propulsion offers the choice of specific impulses covering the complete range from that of the chemical rocket up to that of the photon rocket, with jet speeds close to the speed of light. However, the combination of the

powerplant required to convert nuclear heat to electricity and the space radiator required to radiate away the waste heat are heavy. Hopefully, this powerplant weight can be offset by the saving in propellant associated with the higher specific impulse capability. This suggests that electric propulsion will be of most interest for challenging missions requiring a high Δv; in other words, long time missions requiring a very large fuel load for more conventional propulsion systems.

The heaviness of the power generating plant assures that accelerations of the spacecraft propelled by electric propulsion will be very low - on the order of 10^{-4} g. The electric rocket must thus be launched into orbit by some other propulsion system - probably the chemical rocket.

Once in orbit, the continuous application of thrust will add considerable energy to the space vehicle. The spiral path of a ship with a thrust of one pound for every 10,000 pounds of weight is shown in slide 22. The Moon's orbit is reached in 83 days. Escape from Earth's gravitational energy occurs in 127 days. And with even this low but continuous thrust, faster trips could be made to the edge of the solar system with electric propulsion than with other propulsion means.

The primary reason for seeking high specific impulse is to reduce the jet fluid consumption and hence, the required fuel load for a given space journey. The jet consumption rate is $m = F/I$. (The thrust is now written in weight units.) The fuel load for a propulsion time t is therefore

$$W_f = \frac{F}{I} t \tag{11}$$

On the other hand, the weight of the power generating equipment will increase with the required power output. The powerplant weight is

$$W_e = \frac{\alpha}{\eta} P = \frac{\alpha I F}{45.9\ \eta} \tag{12}$$

where α is in pounds per electric kilowatt and η is the efficiency of converting electrical energy to jet energy. The weight of the powerplant plus propellant is thus

$$W = W_f + W_e = \frac{F}{I} t + \frac{\alpha I F}{45.9\ \eta} \tag{13}$$

These weights are shown schematically on slide 1.

The minimum weight to thrust ratio is obtained when

$$I^2 = \frac{45.9\ \eta t}{\alpha} \tag{14}$$

Thus, propulsion time is always involved as well as specific powerplant weight when choosing the right specific impulse for a mission. Now the payload plus structural weight is equal to the total weight minus the sum of fuel plus powerplant weight

$$W_{p+s} = W_o - W_f - W_e \tag{15}$$

Inserting I from (14) into (13) and the resulting $(W_f + W_e)$ into (15) gives

$$\frac{W_{p+s}}{W_o} = 1 - 2\frac{F}{W_o}\sqrt{\frac{\alpha t}{45.9\ \eta}} \tag{16}$$

Slide 23 shows the payload plus structural weight fraction that can be carried from a 300-mile orbit to a stationary orbit, to Moon missions, and to Mars missions, all one-way trips. This figure was computed using optimum impulses for each journey and ratio of α/η, taking into account the loss in ship weight as the journey proceeds. Hence, the overall thrust to weight ratio varies somewhat along each curve. For the Mars journey, there is a coasting period following the thrusting portion of the flight. Clearly, larger payload plus structural weight fractions can be carried for the longer propulsion times on each mission. Also, higher powerplant specific weights are allowed for a given payload fraction on long missions than for short. In general, the lower the specific weight, the better the performance. Much more sophisticated and more exact treatments of electric propulsion missions are, of course, in the literature. The optimized interplanetary flights of Irving and Blum, for example, require variable specific impulses along the flight trajectory. For best performance, the electric powerplant should be operated at its maximum output. Maximization of the payload fraction by means of the calculus of variations subject to this constraint requires that the propellant mass flow rate, the thrust, the specific impulse, and the thrust divided by the spaceship weight all vary with time along the trajectory. The variation in specific impulse for optimized flight is shown on slide 24 as a function of the mission time passage. You may see that substantial specific impulse variations are required for optimized performance. However, it should be noted that in the region of the peak during the time period from 40 to 60 days, the thrust would be low. Hence, the use of smaller specific impulses during this time period might not compromise the payload greatly.

Optimum Vehicle Design parameters for Irving-Blum trajectories have been computed by Melbourne and are presented in slide 25. Plotted is the payload mass as a function of the total propulsion system mass fraction. The quantity α_{ps} is the total propulsion system specific weight, a is the thrust divided by the total vehicle mass and τ is the propulsion time. The plot only covers the heliocentric phase of the flight plan. The dotted curve has been drawn through the loci of maximum payload fractions for each value of the parameter $\sqrt{\frac{\alpha_{ps}}{2}\int_o^\tau \frac{a^2}{\eta}\,dt}$. Clearly, the total electric propulsion system should not weigh more than 26 percent of the initial gross weight. The lower the propulsion system specific weight, the higher will be the payload fraction.

With these preliminary remarks, let us proceed to the discussion of electric propulsion hardware. I plan on dividing my discussions in two parts, one on accelerators and the second on power generation equipment.

Electric propulsion accelerators. - Three types of electric rockets have been defined as shown on slide 26. They are:

(a) Ion accelerators: propulsion by means of charged particles that have been accelerated by electric fields

(b) Plasma accelerators: propulsion by means of a plasma that has been accelerated by combination of electric and magnetic fields

(c) Electrothermal accelerators: propulsion by means of a fluid that has been heated by electricity and is then expanded through a more or less conventional supersonic nozzle. I will discuss the electrothermal accelerators first

The heating may be accomplished either in an electric arc or by means of a resistance heater. In either case, the performance is limited by the ability of materials to be cooled.

The arc heated rocket is shown schematically on slide 27. The propellant, probably hydrogen, is used to regeneratively cool the nozzle and electrodes. The propellant then passes through the arc to the exhaust nozzle and to space. The arc is generally stabilized either by injecting the propellant into the heating chamber in a vortex flow or by the use of magnetic fields. A ballast resistor may be required between the generator and the arc chamber to promote further stabilization.

Experimentally, the arc-heated rockets are running at specific impulses below 2000 and at efficiencies of perhaps 60 percent. One hundred percent efficiency is, of course, out of the question because of the nonequilibrium lack of recombination of the dissociated propellant in the exhaust nozzle.

The resistojet is shown in slide 28. In this arrangement, the propellant is energized by an electrically heated tungsten resistance. Hence, a maximum specific impulse of perhaps 1000 is feasible. The specific impulse on electrothermal rockets roughly follows equation (4).

The electrothermal rockets are useful for attitude control and for near-Earth missions where the specific impulses of the electrothermal rocket are near optimum. The electrothermal rocket can also be justified for missions where the electric powerplant is already on board the spacecraft for other reasons. In this case, the propulsion system would not be charged with the weight of the power supply. (A communication satellite, for example.) However, the "pure" electrothermal rocket that simply uses electric energy to heat the propellant is not competitive with the nuclear rocket or with ion propulsion for that matter, on deep space missions.

This latter conclusion follows from a consideration of the powerplant. You see, nuclear reactor heat is converted to electricity by direct or indirect means at no more than 20 percent efficiency. Hence, at least four times the required power must be radiated to space in a radiator that is

both cumbersome and heavy. It does not make sense to convert nuclear heat to electricity in order to produce heat at such a weight penalty. Hence, electric propulsion is, in general, not competitive at specific impulses less than about 2000 with the simpler open cycle nuclear rocket. This is just the specific impulse range of the "pure" electrothermal devices.

These conclusions do not apply to the hybrid plasma arc accelerators that employ MHD forces in the arc to accelerate the plasma. Such devices studied by the Giannini Scientific Corporation, Avco, and Electro-Optical Systems, Inc. are yielding specific impulses as high as 10,000 with efficiencies quoted as high as 60 percent or more. These will be discussed briefly later.

Ion accelerators. - An ion rocket, slide 26, contains a source of positive ions, a set of electrodes for accelerating the ions, and an electron source for neutralizing the beam following the acceleration. The beam leaving the engine must, of course, be electrically neutral if thrust is to be maintained.

The jet velocity of the ion source is related directly to the voltage drop across the accelerator portion of the engine. If the gain in kinetic energy of a charged particle $\frac{1}{2}$ mu^2 is equated to the change in potential energy $\eta e\varphi$ with some juggling of units, we obtain the specific impulse as

$$I = 1.42\times10^3 \sqrt{\frac{\eta\varphi}{W}} \qquad (17)$$

where φ is the potential drop across the accelerator in volts and W is the molecular weight of the propellant. η is the number of electron charges on the particle. By comparing this relation with equation (4) obtained earlier, you can easily see that temperature and voltage are interchangeable. For singly charged hydrogen molecules, one volt of acceleration would give a specific impulse of about one thousand. Thus, a great range of specific impulses are possible simply by adjusting the potential drop across the accelerator.

On the other hand, there are fundamental limits to the beam currents of an ion accelerator. If too many charges of like sign try to pass simultaneously through the accelerator, then the electric field due to the ion cloud is opposed to the field due to the accelerator potential. Thus, the intensity of an ion beam is generally limited by space charge considerations in accordance with the Langmuir-Childs relation:

$$i = 5.56\times10^{-12} \sqrt{\frac{\varepsilon}{\mu}} \frac{\varphi^{3/2}}{L^2} \qquad (18)$$

where ε/μ is the charge to mass ratio in coulombs per kilogram, φ is the potential in volts, and L is the distance from the ion source to the accelerator grid.

There is, of course, the possibility of using higher acceleration voltages than required for the optimum impulse, followed by a deceleration electrode to bring the impulse back down to the required value. This accel-

decel trick gives an improvement in beam current density over the conventional limit set by equation (18).

If accel-decel is not employed, the thrust per unit area may be obtained by Newton's laws combined with equation (18):

$$\frac{F}{A} = 8\times10^{-13}\left(\frac{\varphi}{L}\right)^2 \approx 1.8\times10^{-9}\left(\frac{\mu}{e}\right)^2 \frac{I^4}{L^2} \qquad (19)$$

Thus, if the specific impulse is fixed by the mission, the thrust per unit area increases with the square of the mass to charge ratio. Hence, the desire for high molecular weight ions. Thus, the thrust density is set by the mass to charge ratio while the specific impulse is adjusted by means of the accelerator voltage within voltage breakdown limits.

Following release of the positive ions at optimum impulse and ground potential, electrons should be blended with the beam as soon as possible to neutralize the charge. The electron velocity should equal the ion velocity. The acceleration voltage of the electrons should therefore be smaller in proportion to the mass ratio than that of the ions. The mass ratio of an electron to a cesium atom is 4.12×10^{-6}. Hence, a 10,000 electron volt cesium ion would have the same speed as an 0.04 volt electron. This low energy represents an electron at a temperature of only 4° F. Hence, all that is required for beam neutralization is to place a hot electron emitting filament in the beam downstream of the accelerator. With almost insignificant loss in the positive ion energy, the electrons are simply dragged along by the positive charges to produce beam neutralization.

Slide 29 shows a schematic diagram of a cesium ion engine. Cesium gas is first produced in a vaporizing chamber. It is then brought into contact with hot tungsten surfaces. In early experiments, the tungsten surfaces were composed simply of a labyrinth of tungsten strips. In most of the modern engines, porous tungsten is used through which the cesium gas passes.

The ionization potential of cesium is 3.87 volts. This represents the work required to remove an electron from the cesium atom. On the other hand, the work function or the containment energy of electrons in tungsten is higher than 3.87 volts. Hence, each atom of cesium is ionized as it bounces off a tungsten surface. The tungsten must be kept hot simply to keep the surface clean and free from cesium condensation. A layer of cesium only a few molecules thick would stop the ionization process.

The ions are then accelerated and focused in the accelerator portion of the engine. Acceleration and deceleration electrodes might be employed with the last electrode at essentially space (or ground) potential. Finally, an electron-emitting filament is included to neutralize the ion beam.

Reasonably high vacuums must be used in the evaluation of ion engines. Even at 10^{-5} Torr, there is a sufficient supply of neutrals so that charge exchange can occur in the beam between neutrals and ions. This leads to beam defocusing and electrode erosion due to sputtering. As a matter of fact, the beam will neutralize itself without the aid of the electron-emitting filament at these pressures. Hence, facility pressure should be on the order of 10^{-6} Torr or better.

Slide 30 shows an ion beam in one of our Lewis Research Center tanks. This photo is slightly faked in that under high vacuum conditions, the beam is invisible. For this picture, we raised the tank pressure enough so that the ion bombardment of the neutral background gas produces the glow.

The electron bombardment ion engine invented by Harold Kaufman at the Lewis Research Center is shown on slide 31. In this engine, the ionization is produced by electron bombardment. The electrons are emitted from a filament along the axis and are attracted to the outer concentric cylindrical shell by a positive voltage of, say, 100 volts. An imposed axial magnetic field, however, forces the electrons to gyrate around the field lines in epicycloidal paths around the axis. Mercury ions are produced by electron bombardment in this annular ionization region. They drift from here through the discharge ports to be accelerated toward space. Successful electron bombardment engines have been produced using permanent magnets in order to minimize the power losses. They have also been run successfully using either mercury or cesium as the propellant. The largest engine run so far at Lewis has a beam 1/2 meter in diameter.

The efficiency of several thrustor types are compared in slide 32. Generally speaking, thrustor efficiency improves with increasing specific impulse simply because the beam energy is increasing while the losses remain unaltered. On the contact ionization engine, the principal loss is associated with the requirement that the tungsten ionizer be kept hot. This engine is thus severely penalized for specific impulses below five or six thousand but performs quite well at values on the order of 20,000 seconds or higher. For this engine, the ionization mass fraction is essentially 100 percent.

On the other hand, the inherent losses for the electron bombardment engine can be relatively low. The most difficult problem is to keep the ionization mass fraction of expelled atoms above about 80 percent at the same time. Nevertheless, tests of a 50 cm diameter engine at the Lewis Research Center have yielded overall efficiencies of 88 percent at a specific impulse of 9000 seconds. No other ion engine has done as well. Experiments are now proceeding with a $1\frac{1}{2}$ meter diameter engine, probably the world's largest.

I also show on this chart an estimated performance curve for colloidal particle accelerators. Experiments on these engines are so preliminary that we really don't yet know what performance can actually be obtained. You will recall from equation (19) that the thrust per unit area is proportional to the square of the mass to charge ratio ($\mu/\mathcal{E}$). Also, if the mass to

charge ratio is very high, then the acceleration voltage will be very high. The idea is to produce colloidal particles of fractional micron dimensions, spray charges on them, and accelerate them to space taking care to neutralize the beam. If the charged mass fraction can be upped to nearly 100 percent and if the particles all have essentially the same mass to charge ratio, then the kind of performance shown can probably be achieved. Time and more research will tell.

At Lewis, we are producing the colloidal particles in a condensation shock generated by flowing vaporized aluminum chloride through a supersonic nozzle (slide 33). Charges are then sprayed on the colloidal particles thus generated either by corona discharge or by electron bombardment. The actual hardware for these two arrangements is shown in slides 34 and 35. I won't say much more except that the preliminary results we have obtained are encouraging for low specific impulse engines. Some other laboratories are studying the charging of aerosol sprays to accomplish the same desired performance.

Another potential ion source for electric propulsion (slide 36) is due to Von Ardenne. This source utilizes an electric arc to ionize the jet. The arc electrons proceeding forward from the filament are reflected by the positive ion accelerating field. They are also confined to a region near the axis by an intense magnetic field in a Phillips ion gage arrangement. In the Phillips ion gage, electrons are confined to move axially by means of an axial magnetic field. They are accelerated from an electron emitting filament toward a plasma region by means of an axial electric field which reverses in polarity on the opposite side of the plasma region. The electrons then accelerate toward the plasma region, pass through, and are reflected back into the plasma region from the opposite side, making many reverberations back and forth. The electrons produce positive ions through bombardment and neutralize the space charge effects in the plasma region. The positive ions so formed are accelerated out of the plasma region by means of the axial electric fields. Thus, the electron bombardment of the propellant in the arc gives nearly 100 percent ionization and perhaps an order of magnitude larger current densities than would be predicted from the Langmuir-Childs space charge limit equation. This latter effect is due to the fact that the ion beam is essentially neutralized in the low voltage or most critical portion of the ion acceleration history.

Still another potential source is the so-called Hall current accelerator (slide 37). In this source, as yet very much in the research stages, ionization is produced by electron bombardment in a region containing an axial electric field and a radial magnetic field. The cyclotron radius of the electrons is small compared to the apparatus dimensions so that the electrons are confined to gyrate on cycloidal type paths on a cylindrical surface about the axis. On the other hand, the cyclotron radius is chosen as large compared to the apparatus dimensions. In this manner, the ions leave the magnetic field before they have an opportunity to complete their cycloidal paths. Like the Von Ardenne arrangement, this source also has space charge neutralization in the low velocity regions of acceleration. Hence, the current density may be much higher than predicted by the Langmuir-Childs space charge limit (equation (8)).

The United Aircraft Corporation has combined a Hall current accelerator with a cesium contact ionization electrode. They thus use the Hall current electrons to neutralize the space charge limit set by the Langmuir-Childs equation. Higher ion currents than the equations predict were obtained on preliminary experiments.

Plasma accelerators. - Plasma accelerators are the third type listed on slide 26. A plasma is an ionized gas containing equal numbers of positive and negative charges - and hence is on the average electrically neutral. This plasma can serve as a conductor and hence can be accelerated by electromagnetic forces.

Now, both positive and negative charges will spiral around magnetic field lines as shown on slide 38. If an electric field is superimposed, the charges will alternately accelerate and decelerate with corresponding changes in path curvature. As a result, both positive and negative charges move through space in the same direction with an average drift velocity:

$$\bar{u} = \frac{\bar{E} \times \bar{H}}{H^2} \tag{20}$$

where $\bar{E}$ and $\bar{H}$ are the electric and magnetic field vectors, respectively. This drift velocity corresponds to the zero power or idling speed of a motor. If energy is to be added to the plasma, the electric field vector must be tilted toward the direction of the desired acceleration. Accelerators (slide 39) utilizing these crossed electric and magnetic fields are called $\bar{E} \times \bar{H}$ accelerators. Space charge neutralization is, of course, unnecessary in plasma accelerators since both positive and negative charges move in the same average direction and with the same speed.

A second type plasma motor may be visualized by having the plasma serve as a conductor in a magnetic field. The force on the plasma is then

$$\bar{F} = \bar{J} \times \bar{H}$$

where J is the current. Now, a current can be generated by positive charges moving in one direction and negative charges moving in the opposite sense. Hence, here again, both positive and negative charges on the average move together so that space charge neutralization is unnecessary.

A simple form of a plasma motor is shown on slide 40. An arc is struck between two parallel conductors. The resulting current generates a magnetic field that propels the plasma arc along the rails. The favored geometry for rail accelerators utilizes coaxial conductors with electric current flowing radially through the plasma. In this arrangement, the solenoidal magnetic field is generated by the current flowing in the central conductor. This reacts with the radial current to produce an axial force.

Earlier mention was made of the hybrid plasma arc which can produce specific impulses much higher than conventional electrothermal accelerators. The hybrid arc depends on the axial component of the $\bar{J} \times \bar{H}$ force for its

energy. This component can arise either through a radial current interacting with a solenoidal magnetic field or through a solenoidal current interacting with a radial magnetic field. Thus in cylindrical coordinates:

$$(\bar{J} \times \bar{H})_z = J_r H_\theta - J_\theta H_r \qquad (22)$$

Accelerators that depend upon the first and second term of equation (22) are called $J_r H_\theta$ and $J_\theta H_r$ types, respectively.

The coaxial gun is a $J_r H_\theta$ type accelerator. One can imagine that the central electrode could be replaced by a conducting plasma operated in the high current or arc mode. The magnetic pressure would pinch the plasma toward the axis to maintain a semblance of the coaxial geometry. If propellant is fed through this arc, it will be ionized and accelerated as in the coaxial gun. You can thus see why the $J_r H_\theta$ hybrid arc gives high specific impulse.

Likewise, a radial magnetic field in conjunction with an axial electric field will produce a solenoidal Hall current as we have seen. This current can then react with the radial magnetic field to produce an axial force. If an arc is maintained between the electric field electrodes, it will promote ionization of the propellant. Geometries may be visualized to incorporate both $J_r H_\theta$ and $J_\theta H_r$ forces simultaneously. However, this approach to electric propulsion is so new that a basic understanding of the processes that go on in the accelerator is still lacking. Transient rather than steady state processes, for example, may also be involved.

The magnetic pinch effect may also be used to obtain magnetic plasma projection, one form of which is shown on slide 41. An arc is struck as a continuation of the center conductor of a coaxial cable. The pressure associated with the confining magnetic field of the current carrying plasma plows the plasma toward the axis during the condenser discharge to give extreme pressure and temperature. The plasma squirts out through the hole on the axis. You may also note the resemblance of the current paths for this device and those of the coaxial gun and the $J_r H_\theta$ type hybrid arc.

A magnetic mirror may also be used for trapping and projecting plasma. In a magnetic mirror (slide 42) the plasma is trapped in the magnetic trough between regions of higher field strength. If the "mirror" is then shifted along the axis at a continuously increasing speed to the desired plasma projection velocity, the plasma will also be accelerated accordingly as a surf board rides the waves. Instead of actually shifting the magnetic mirror axially, a similar effect is obtained by the proper phasing of the alternating field strengths from each coil.

You can see that there are many ways to accelerate plasma - almost any form of linear motor where plasma replaces the conductors will serve. I haven't even mentioned the AC self-induction schemes.

Most of the plasma propulsion ideas are not yet competitive with ion rockets. The efficiency is either too low or the hardware is too heavy.

Nevertheless, many experts believe that the day will come when ion sources are obsolete. Combined ion and plasma sources, such as the Hall current accelerator, may well be better than either alone. In any case, a great deal of progress must be made before the propulsion world will get excited about plasma sources. On the other hand, electric propulsion looks most promising for missions requiring high specific impulse. For such missions, two sources are almost to the usable stage of development now - the cesium contact ionization source and the Kaufman electron bombardment engine. The power production system is much more likely to delay the practical use of electric propulsion than would the accelerator.

Power Generation Systems

We have stressed earlier that electric propulsion systems were heavy; but because of the high specific impulse capabilities, the savings in propellants on an extended space mission would more than compensate for the powerplant weight. The competitive status of electric propulsion therefore depends upon how lightweight the powerplant can be, as well as its endurance capability to remain operable throughout the extended space mission.

Slide 43 compares the gross weight required in orbit on a manned Mars mission for the nuclear rocket and electric propulsion. Clearly, longer mission times or lighter specific powerplant weights make electric propulsion more competitive. The challenge is to produce powerplants with specific weights less than about 20 pounds per kilowatt with proven reliabilities for time periods on the order of 500 or 600 days.

Unfortunately, this low specific weight has not been approached by any power system currently under development. Even if the basic powerplant were sufficiently light, the weight and inefficiencies of all the components can add considerably to the effective weight of the electric propulsion system. This growth in weight is illustrated in slide 44, which includes only one of many cases discussed by Mickelsen in NASA TM X-52041.

The basic powerplant was assumed to weigh 22 pounds per kilowatt of shaft power. The generator weighs only 1 pound per kilowatt, but the generator inefficiency requires that the basic powerplant be increased in size by the growth factor $1/0.92 = 1.09$, so that the effective weight of the generator is 2.9 pounds per kilowatt. Similar weight growth occurs for each component successively up to and including the thrustor. For this table, the basic power conditioning weights assumed the extremely optimistic value of 2.1 pounds per kilowatt based on operation at 700° F. Even so, the overall weight growth of this powerplant system was from 22 up to 40 pounds per kilowatt.

The requirements for several missions are shown in a different manner on slide 45. The largest specific powerplant weight for the electric rocket that will remain competitive with the nuclear rocket is plotted as a function of trip time. Electric rockets are superior to nuclear rockets if the specific powerplant weights are lower than the curve. Even though there is no universal curve, it is clear that longer trip times permit higher specific

powerplant weights. However, the reliability requirements become more extreme. Now, one can imagine that reliability could improve if powerplant weight is allowed to increase. One could then superimpose a curve of endurance time on this one as a function of powerplant weight. The optimism for electric propulsion then is described by these limiting curves. If the powerplant specific weight is too high or the endurance is too poor, then electric propulsion would lose its competitive status.

A combined nuclear-rocket and electric propulsion system may be superior for a manned Mars mission to either one by itself. Slide 46 (from MacKay, AIAA paper no. 64-498) shows this superiority of the combined system for a seven-man Mars mission for trip times less than 500 days. For this comparison, a perhaps unrealistic specific powerplant mass of 15 pounds per kilowatt was assumed.

The combined nuclear-rocket and electric propulsion system will also competitively allow the use of higher electric propulsion specific powerplant weights. In slide 47 (from Mickelsen and MacKay, Astronautics and Aeronautics Journal, Jan. 1965) the payload mass fraction for a general mission is plotted as a function of the specific weight of the electric propulsion system. Clearly, larger payload fractions can be obtained for the combined system even with specific weights as high as 40 or 50 pounds per kilowatt as compared with the all-nuclear 420-day trip. The all-electric system of this study is competitive with all-nuclear propulsion for powerplant specific weights somewhat higher than those in slide 43 which used different mission assumptions.

Let us dwell for a moment on this question of endurance. One year has about 8800 hours so we are asking for at least 10,000 hours of trouble-free operation. An automobile would travel 300,000 miles at 30 miles an hour in that time. Surely some trouble would be expected. So our space powerplant must be much better than our automobile. On the other hand, turbojet engines have been run for 4000 hours without overhaul, as have the rotating machinery components for the mercury-vapor Rankine-cycle Sunflower Spacepower System. In other words, the long running times required are not necessarily insurmountable. This long time reliability, however, must be achieved with very lightweight hardware.

The Rankine cycle diagramed on slide 48 might be able to match the weight requirements for electric propulsion. In this cycle, liquid metal (perhaps lithium) circulates through the reactor loop carrying heat to the heat exchanger. A second liquid metal, such as potassium, is vaporized in the boiler to carry energy to the turbine. The radiator condenses the gaseous metal vapor from the turbine and the pump rebuilds the pressure level of the liquid metal entering the boiler. The turbine drives the generator producing electric power.

The overall efficiency of the Rankine cycle is probably not more than 20 percent. Hence, at least 80 percent of the heat generated by the reactor must be radiated to space.

The heaviest component of an electrical power generating system is the radiator for eliminating the waste heat. It is also the most vulnerable to meteoroid damage. The radiator for a 10 megawatt system might weigh four or five pounds per kilowatt if it did not have meteoroid protection. With protection, the weight might be as high as 20 or 30 pounds per electric kilowatt for the long time missions. Because the area of the radiator is strongly temperature dependent, being approximately proportional to the fourth power of the absolute temperature, there is a strong temptation to run the system at the highest possible temperature to reduce radiator area and hence, system weight. The limiting temperature is set by material corrosion difficulties for which liquid metal systems are notorious. High temperatures imply refractory metal loops that are very sensitive to oxygen contamination in terms of parts per million. Oxygen can diffuse through the refractory metal from the outside to cause corrosive deterioration. Hence, liquid metal loops or space power systems must either be developed in a vacuum system or under an inert atmosphere such as argon. Hence, the developmental problems are not easy.

Corrosion problems are also characteristically strongly temperature dependent. If the temperature could be lowered, corrosion problems are greatly alleviated.

The possibilities of using lightweight material might also raise the question of how high one should increase the radiator temperature in spite of the heat transfer dependence on T^4. A beryllium radiator, for example, could feasibly be operated at 1400° F. Beryllium is one-fourth as heavy as conventional high-temperature materials. Thus a "conventional" high-temperature radiator would have to operate quite a bit hotter to break even with beryllium on a weight basis. Beryllium, on the other hand, may have unacceptable fabrication problems. Or perhaps the radiator tubes might shatter under meteoroid impact, or launch vibration conditions. So the beryllium radiator is still speculative.

There is also a considerable uncertainty in the survival probabilities for radiators in space. That survival will depend not only upon position (i.e., near Earth, near Mars, etc.) and time in space, but also on the radiator orientation relative to the plane of the ecliptic, its material of construction, and its design. Even near Earth, a meteoroid damage experiment in space would have to be exposed for a large area-time product to give dependable data for spacecraft design. Assurance of a 99 percent survival probability with a 50 percent confidence interval requires, for example, that the experiment have an area-time product 1600 times as large as the evaluated spacecraft. Clearly, such experiments are unrealistic for the already large radiators, say 20,000 square feet, of an electric-propulsion system. Nevertheless, some data such as shown on slide 49, has been obtained by Explorer XVI. These data suggest that a 10,000 square foot radiator with armor protection of 0.01-inch stainless steel would receive a penetration every 10 days. Armor protection of 0.1 inch on each exposed external surface would have about one penetration every three years.

Meteoroid damage is more probable with large surfaces than with small. Hence, the specific weight of a space radiator (i.e., lb/kw) increases roughly as the power level or the exposure time to the one-third power. Other specific weights tend to decrease with increasing power level. Hence, there is a design power level somewhere around one megawatt where minimum specific weights will be achieved. The actual value, of course, depends upon which meteoroid damage criterion is chosen.

If segmented radiators are used, systems lighter than this optimum can be obtained with no change in survival probability. This effect is shown on slide 50 where the relative weight of a radiator system is plotted against the number of segments. Segmentation holds a further advantage in that the power-generation system may continue to operate at a reduced power level after being damaged. For this particular example, the reduced radiator effectiveness is limited to 0.75 of the original heat transfer capacity.

The vulnerability of the space radiator to meteoroid damage results in part from the extensive exposed areas of liquid filled passages. Unconventional geometries, such as the so-called belt radiators shown in slide 51, have been proposed to alleviate these difficulties. In the radiator proposed by Weatherston of the Cornell Aeronautical Laboratory, an endless belt passes over a rotating primary heat transfer cylinder. This belt provides the area expansion that permits the heat to be radiated to space. In Rocketdyne proposals, the belt progresses in caterpillar fashion around a stationary heat transfer cylinder. Presumably, a puncture of the belt would not cause undue difficulties.

However, the belt radiators are not without difficulties. The guiding rollers would certainly have lubrication difficulties; and the belt flexing and rolling may adversely affect the structural life. Even more fundamental is the problem of maintaining high heat transfer between the belt and cylinder in the space environment. Under the outgassing high-vacuum conditions of space, one of the major heat-transfer mechanisms - that of the thin convection gas film that normally adheres to the belt surfaces - may be lost. Data obtained by Sommers and Coles at the Lewis Research Center have, in fact shown that under vacuum conditions heat transfer rates are perhaps a factor of 20 too low. The use of liquid tin or gallium on the belt surface could bring this heat transfer up to usable levels. However, the belt temperature must then be kept at a value low enough to prevent significant evaporation of the coating.

The radiation amplifier, slide 52, is another approach. Here the primary fluid filled radiator segments are folded over themselves so that only the outside tubes need to be protected. The heat from the tubes inside the folds is carried to space by means of thin disks or belts operating at perhaps half the primary radiator absolute temperature.

The heat pipe is still another approach to minimize the required exposed area of radiator tube filled with primary fluid. A tube and fin radiator may be imagined containing hollow fins. The segmented fin cavities would contain a boiling and condensing fluid. The fluid boils on the radiator tube and condenses on the fin. The condensed liquid is conducted back

to the tube by means of a capillary wick. In this manner high heat-transfer rates to the fins can be maintained giving fin temperature approaching those of the primary fluids. A meteoroid puncture of a fin compartment produces only local damage. The fins can also be arranged to serve as bumpers to protect the fluid tubes.

Now, inefficiencies in any part of the power generating system will obviously produce more waste heat for the radiator. Likewise, if the system temperature is lowered, the radiator area must be increased.

Slide 53 presents the effect of turbine inlet temperature on relative radiator area. More than a four-fold difference in area exists between turbine-inlet temperatures of 1200° and 2000° F. This fact indicates the need for high system temperatures to maintain low system weights - hence, the use of alkali metals and refractory-based alloys.

As turbine efficiency, slide 54, increases from 50 to 100 percent, radiator area decreases by a factor of $2\frac{1}{2}$. In view of the heaviness of the radiator, it is apparent that high-performance turbines are a prerequisite to lightweight systems.

The condition of the vapor entering the turbine also has an important effect on radiator weight as is shown on slide 55. The vapor can either be superheated above its boiling temperature or it can be saturated at the entrance to the turbine. If it is saturated, condensation will occur as the pressure drops during the turbine expansion process leading to wet-vapor operation of the turbine. Such operation might cause many design problems such as erosion and fatigue if good performance and high reliability are to be achieved. Nevertheless, reducing the turbine moisture at the exit from 14 to 4 percent by use of superheated vapor, increases the radiator area by a factor of 1.5. Therefore, it appears desirable to use nearly saturated vapor at the turbine inlet, if possible.

There are many other tough engineering problems that must be solved to produce a reliable Rankine cycle lightweight space power system for electric propulsion. These include all those problems connected with liquid metal erosion and corrosion, with sludging and radiator clogging associated with material transfers; difficulties of obtaining reliable turbine materials; bearings lubricated by liquid metals; seals to contain the fluids; cavitation in the pump; condensation and fluid distribution problems in the radiator under zero "g" conditions, and with probable restart difficulties associated with freezing and sludging in the tubes. Some of these would necessarily have to be evaluated via costly space experiments. And I have not mentioned any of the problems associated with the reactor or with the difficulties of launching cumbersome radiators and of maintaining fluid system integrity against leakage of the liquid metals to space. With all of these difficulties, the Rankine cycle powerplant development will be neither easy, nor quick, and it likely will be very expensive. Secondly, with so many difficulties and unknowns, achievement of the required reliability will be a long time in coming. Nevertheless, the Rankine cycle high temperature liquid metal systems hold greater

promise than most other approaches toward the achievement of lightweight space power for electric propulsion.

Rankine cycle steam powerplants have also been proposed by the Astra Corporation. They look promising at the moment, but the studies are very preliminary.

Many of the listed difficult engineering and materials problems associated with two-phase liquid metal systems can be avoided by utilizing the all gas Brayton cycle diagramed in slide 56. Using an inert gas such as neon or argon, most of the corrosion problems vanish. Hence, higher temperatures can perhaps be utilized in the cycle. The unit could be canned, thus eliminating the problems of seals on the alternator. The use of gas bearings might lead to a system with almost indefinitely long time reliability, and shutdown and restart should be easier than on a Rankine cycle powerplant. What's more, we have a wealth of technical and engineering experience on Brayton cycle machinery from the turbojet and turboprop engine studies.

On the other hand, the radiator on the Brayton cycle is bulky. There must be a large temperature drop across the radiator to keep the machine running. Because radiation to space follows according to T^4, the low temperature portions of the radiator are very much less efficient than the high temperature portions. Hence, to really capitalize on a Brayton cycle system for electric propulsion would require operation at much higher temperature levels than we are accustomed to considering in order to keep the specific weight down to usable values. With inert fluids such as neon, higher temperature can certainly be visualized. However, this means a new reactor development that might also be beyond our current technology.

Creep and stress rupture considerations on materials suggest a top reactor fuel element temperature of 2800° to 3000° F for 10,000 hours of life. This would probably be a fast reactor. Perhaps turbine inlet temperatures of as high as 2500° F, could then be considered. Such a system would have specific weights sufficiently low to be attractive for electric propulsion - on the order of 15 to 30 pounds per kilowatt. At 2040° F inlet to the turbine, the specific weight has been estimated by Stewart of the Lewis Research Center in preliminary analyses at about 25 pounds per kilowatt or higher.

Some discussion should be included on the status of thermionic-converter space power systems. The thermionic converter boils off electrons from the emitter, which then progress to the collector (slide 57). In this manner, heat is directly converted to electricity by differences in temperature and work function between the emitter and the collector.

The power level of the vacuum thermionic converter is, of course, space-charge limited. Therefore if reasonable spacing between cathode and anode is employed, an easily ionized gas such as cesium must be inserted to neutralize the electronic charge. The resulting "plasma thermionic converter" has received considerable interest as a potential source of space power.

The theoretical Carnot efficiency of the plasma thermionic converter ranges from 25 to 50 percent. Experimental efficiencies have been about one-third of these values, or a maximum of about 17 percent. The remaining heat energy must be discharged to space by means of a radiator. Unfortunately, the higher efficiency occurs with the lowest anode temperature which suggests a larger radiator. When the system weight including the radiator is minimized, the efficiency is approximately 10 percent, or perhaps a little higher with the new meteoroid data.

When we decide to use the thermionic converter in a space power system, we must decide whether to install the elements in pile or in an out-of-pile arrangement. The out-of-pile design is much easier and straightforward. A liquid metal or gas loop would carry reactor heat to the individual cathodes. However, the limiting temperature of the liquid metal system occurs in the reactor with the cathode at a still lower temperature. In this arrangement, there is perhaps a 600° F penalty on the maximum cathode temperature leading to estimated system weights so large that we may draw the conclusion that out-of-pile thermionic conversion systems are not interesting for electric propulsion at this time. The conclusion depends strongly on the maximum feasible temperature of the system. The higher the temperature, the more feasible the out-of-pile arrangement.

A schematic diagram of an in-pile thermionic converter system is shown on slide 58. In this configuration, the cathode on each thermionic unit is fueled with uranium. The reactor then consists of an array of thermionic elements arranged into a critical assembly of fueled hot cathodes. The anodes must, of course, be cooled. Thus, the reactor and the power generation equipment are combined into one unit.

Perhaps ninety percent of the energy so generated must be carried to the space radiator by means of a working fluid. Because the converter is a high-temperature device, the anode cooling and the transfer of heat to the radiator are accomplished by a liquid-metal system. Hence, the thermionic converter has the same limitations on performance due to the use of liquid metals as the Rankine cycle rotating-machinery device. The thermionic converter may operate at higher temperatures - turbine inlet temperature corresponds to anode temperature - but gains from this difference are offset at present by the lower efficiencies of the minimum-weight diode system.

Studies have been conducted on the use of gaseous cooling of the anode to raise the operating temperatures. In these studies, the pumping power to circulate the cooling fluid was unreasonably large except when large temperature drops across the radiator were employed. Then the radiator became both large and, with meteoroid protection, too heavy. Hence, gas-cooled thermionic conversion systems currently are not interesting for electric propulsion.

For that matter, no one has yet designed a satisfactory liquid-cooled thermionic power system for space. One might propose a reactor composed of a critical assembly of thermionic diodes, each with its uranium-fueled cathode. The engineering problems associated with balancing the nuclear

characteristics of such a reactor with the diode thermal and electrical requirements, including the multiplicity of series and parallel groups of diodes, each cooled with a properly insulated liquid-metal system connected to a common radiator, is challenging to say the least. Add to this the requirement for replaceability of each radioactive diode unit upon failure and the problem becomes even more difficult.

Attention should be called to the fact that the power generated by the thermionic elements constitutes an appreciable source of reactor cooling. If an open circuit were to develop, the temperatures in the fueled cathodes of the affected diode would jump perhaps 500° to 600° F. This difficulty is partly alleviated by designing the fueled cathodes on the outside of each element rather than on the inside. This arrangement allows for better heat transfer among the fuel elements, more convenient dissipation of fission gases, easier isolation of cooling passages, etc. so that the temperature jump on open circuit is only 100° to 200° F. Hence, placing the cathode on the outside of each diode is the preferred arrangement.

There is still another major problem with the thermionic system. It requires a relatively heavy power conditioning system to provide the proper voltage and currents for electric propulsion. When engineers are actually faced with the job of designing a complete thermionic system, they may find that the optimistically low estimates of the weights of the thermionic conversion systems sometimes included in the literature will grow to equal or surpass the weight estimates of more conventional approaches. I come to the conclusion that the development of a thermionic system is probably more difficult than the high temperature liquid metal Rankine cycle system.

You can see from this less than optimistic discussion that space power in sizes required for electric propulsion will not come easy. The systems that will provide this power with low enough specific weights and high enough reliability for man-rated interplanetary flights are a long way in the future. Even the basic research so necessary prior to a development phase is moving slowly and with great difficulties and expense. One could easily conclude that manned planetary flights using nuclear rockets are more likely to be undertaken first. Of course, electric propulsion may be used earlier in much less important applications such as guidance and control, satellite orientation, and satellite orbital adjustments.

V. GASEOUS CORE NUCLEAR ROCKETS

The goal of the gaseous core nuclear rocket is to produce specific impulses above 1000 with a thrust to weight ratio on the order of unity or larger. Using hydrogen as the propellant, the exhaust jet must therefore be considerably hotter than the melting point of known materials. The trick is to heat hydrogen in a gaseous uranium reactor without losing too much uranium.

Cost can be used as a measure of the required hydrogen-to-uranium flow ratio. If it costs $200 per pound to place hydrogen in orbit and

$7000 per pound to produce uranium, this hydrogen-to-uranium weight ratio is 35 to 1.

A typical gaseous core reactor might be 10 feet in diameter and 10 feet long. A uranium partial pressure of about 25 pounds per square inch is required to maintain nuclear criticality. The hydrogen pressure should be as high as possible within the limits of reasonable practice.

Let us suppose that 2000 pounds per square inch is reasonable. Then, if hydrogen and uranium flowed through the reactor together, the hydrogen to uranium mass flow ratio would be:

$$\frac{2000}{25} \times \frac{2}{235} = 0.68$$

which is far below the 35 to 1 required. Hence, we must increase the residence time of the uranium relative to the hydrogen by a factor of about $35/0.68 = 51.5$. The struggle to find a good gaseous core reactor concept revolves about this problem.

Let us assume for the moment that we have a good cavity reactor concept. The cavity will surely be surrounded by a thick moderator and neutron reflector as shown on slide 59. Heat will be generated within this moderator due to absorption of neutron and gamma radiation. This heating amounts to about 10 percent of the reactor power and must be removed regeneratively by the flowing hydrogen.

The maximum temperature of the moderator might be 5000° F. Hydrogen at 5000° F would have a specific impulse of about 900 seconds. Since this represents 10 percent of the heat, the jet specific impulse can be perhaps 900 multiplied by $\sqrt{10}$. Thus, a specific impulse of about 3000 seconds becomes an upper limit for the performance of gaseous core nuclear rockets.

The pressure shell to contain the required reactor pressures of 1000 to 10,000 pounds per square inch is sufficiently thick so that no reactor shield is required. Nevertheless, the total weight of the reactor, including moderator and pressure shell, is from 250,000 to 500,000 pounds. Hence, in a mission comparison with more conventional nuclear rockets, the gaseous-core rocket system would likely require a fuel load of more than 500,000 pounds to capitalize on its higher specific impulse. Thus, more than 1,000,000 pounds in orbit would be required just for the engine and fuel load. To this would have to be added the payload and structural weight requirements. You may thus get some feel for the size of the mission before gaseous core nuclear rockets can be justified.

An early suggestion for a gaseous core reactor is shown in slide 59. Tangentially entering hydrogen passes radially inward through a gaseous uranium vortex. Hopefully, the centrifugal forces associated with the heavier uranium molecules would be balanced by the diffusion drag of the inwardly moving hydrogen. The hydrogen would ultimately move along the axis to the exhaust nozzle as shown in slide 60.

Unfortunately, the drag produced by the flowing hydrogen is so great that excessive loss of uranium will occur unless the hydrogen flow rates are limited to very low values. Hence, in a single-tube vortex reactor, only low thrusts could be obtained without excessive loss of uranium.

One way to avoid this difficulty is to use multiple vortex arrangements as are shown in slide 61. Criticality is achieved by the combination of many gaseous uranium cores. These may either be materially separated, as in the upper left diagram, or established by a matrix injection pattern, as shown in the square box drawing. These schemes were proposed by Jet Propulsion Laboratory and Space Technology Laboratories. Both have a major problem of cooling the enclosed hardware.

Instead of passing all of the hydrogen through the uranium vortex to the core as on slide 59, an alternative arrangement is to bypass part of the hydrogen to flow axially outside the uranium cloud to an annular discharge part. The United Aircraft Corporation is studying this arrangement.

The Lewis Research Center's coaxial jet reactor is illustrated on slide 62. The central core of uranium gas would be injected at a much slower speed than the coaxially moving hydrogen. Hopefully, the mixing processes can be tailored to minimize the uranium loss rate. A hydrogen buffer layer would be added with an intermediate velocity profile between the uranium and the outer hydrogen layer to serve this purpose. The hydrogen to uranium velocity ratio should be 50 to 100 or higher for reasonable fuel conservation.

On the other hand, the velocity difference between the hydrogen and uranium layers can be eliminated entirely by using tangential entry and exit of the fluid as shown on slide 63. The cylindrical uranium core is injected through the two end walls with an angular velocity of rotation to match that of the hydrogen buffer layer. The main hydrogen propellant enters and leaves the reactor tangentially. Small quantities of axially flowing hydrogen can be injected in the end walls for cooling purposes and to match the uranium axial velocity component generated by uranium replenishment. The end walls can even be rotated to eliminate the usual secondary flows.

In all of these reactors, the principal heat transfer mechanism to the hydrogen is by radiation, and the hydrogen must be continuously seeded with graphite powders and other materials to absorb the radiant heat before it reaches the containing walls. This is only one of the many very difficult research problems the cavity reactor faces.

In fact, it is real tough to plan meaningful, definitive experiments to evaluate cavity reactor concepts on small scale. There are grave nuclear and fluid mechanic stability problems that might require simulation of the reactor at close to full scale and full power operating conditions. Thus, the research decision to evaluate the feasibility of a cavity reactor concept may require a hazardous multibillion dollar program.

VI. PROJECT ORION

You have all probably had the joy of propelling a tin can into the air by means of an exploding firecracker. A rocket could conceivably be designed to fly by means of a succession of carefully timed firecrackers exploding in the vicinity of that tin can. The ORION concept is similar except that a succession of small nuclear explosions replace the firecracker and a large space-ship resembling a city water tower in size replaces the tin can. Because the ship must withstand the agonies of nuclear explosions, naturally heavy ship-building construction and assembly methods are required. The design must include techniques for minimizing the destructive effects of the strong shock load, high temperature radiation, and other hazards associated with nuclear explosions in the near vicinity of the ship. And if men are on board, they must somehow be isolated from the large periodic accelerations that could result. You can see that such a spacecraft would be heavy - with weights comparable to that of a gaseous core nuclear rocket. Its use would therefore be restricted to large payloads involving requirements for substantial velocity increments.

To make the basic idea appear plausible, imagine that a nuclear bomb explosion converts the bomb material to an expanding gas at, say, 20,000,000° F. In a vacuum, this gas, which is assumed to be expanding uniformly in all directions, could reach an ultimate radial speed from equation (3) of say, 1.8 million feet per second. If a plate of heavy material intercepts and reflects back a portion of this spherically expanding gas, then a force will be exerted on the plate equal to twice the ultimate gas velocity times the mass flow rate. If n bombs of mass m explode per second, the mass flow rate out from the center of explosion is nm which would be the fuel consumption rate. If the plate subtends an angle 2θ from the explosion center, then the mass flow rate hitting the plate will be approximately

$$\frac{nm \sin^2\theta}{4}$$

Hence, the thrust is

$$F \approx \frac{2nm \sin^2\theta}{4} \times 1{,}800{,}000$$

yielding a specific impulse of:

$$I = \frac{F}{nmg} \approx 28{,}000 \sin^2\theta$$

If the spaceship subtends a half angle of 20° to the bomb explosion center, then $\sin^2\theta = 0.115$, giving a specific impulse of about 3200 seconds using these very arbitrary assumptions. So you see, the idea is plausible. Because the project is classified, I am reluctant to say more about Project ORION.

VII. THERMONUCLEAR ROCKETS

In order to release thermonuclear energy, a plasma of light elements must be heated to a temperature of 1 billion degrees Kelvin. At such temperatures, a portion of the ions are moving at sufficient speeds to cause fusion upon collision, accompanied by the release of large energies.

Four frequently considered fusion reactions are shown on slide 64. The amount of energy liberated to each particle is given in million-electron-volt units. One electron volt is equivalent to 11,605° K. The first two reactions occur with equal probability and are between deuterium ions. The third and fourth are between deuterium and either tritium or helium 3, respectively. The difficulty with using deuterium-deuterium and deuterium-tritium reactions is that a large fraction of the energy appears as high velocity neutrons.

At the temperature ranges of interest, only magnetic fields offer promise as a means of confinement. The neutrons are unaffected by magnetic field and are thus lost from the reaction zone. Recovery of this energy in a cooled shield would only complicate a thermonuclear space propulsion system. Hence, reactions liberating charged particles that can be trapped by magnetic fields are preferred.

Deuterium and helium 3 might be provided as the fuel utilizing the fourth reaction. If the reactor temperature is held at a sufficiently high value, the probability of a deuterium helium 3 reaction is much greater than the deuterium-deuterium reaction so that only about 5 percent of the energy would be liberated as neutrons.

The reacting plasma would be contained in a magnetic bottle as shown in slide 65. The charged particles are reflected back toward the reactor interior by the strong fields on the ends. The plasma pressures of more than 1000 pounds per square inch suggest confining field strengths of over 100 kilogauss. These fields would be provided by superconducting magnets to minimize the power losses associated with containment. The field on one end of the reactor would be weaker than on the other end, which would allow propellant to flow through the magnetic nozzle to space.

The cryogenic magnet must, of course, be cooled to low temperatures with a liquid helium system. To minimize the heat load on the magnet due to bremsstrahlung and neutron radiation, shields are provided as shown on slide 66. The thermal capacity of the hydrogen cools the cryoplant and the neutron or "secondary" shield. This hydrogen is ejected by the reactor exit jet. Additional cooling through a radiator system is required for the bremsstrahlung or "primary" shield.

The performance of such a thermonuclear rocket is pretty spectacular. Thrust to engine weight ratios of as high as 0.01 are feasible and correspond to about 1 or 2 kilowatts of jet power per pound of engine weight. The specific impulse would be on the order of 10,000 seconds. The performance of

such a system would therefore be about an order of magnitude better than that predicted for the nuclear fission electric propulsion system. Controlled fusion, however, has not yet been obtained in a laboratory reactor. Hence, the thermonuclear rocket will not be a reality for a long time in the future.

VIII. THE PHOTON ROCKET

The maximum possible value of specific impulse, 3×10^7, is obtained in the photon rocket. In this case, however, the power requirements are so high that no known energy source or conversion method is sufficient. Nearly 2 million horsepower or 1330 megawatts of power would be required for each pound of thrust. Even if such energy sources were available, directing the photons in the jet would require materials with almost perfect reflection coefficients to keep them from overheating.

The photon sail, on the other hand, might be practical for some space missions. The maximum thrust on a photon sail at the Earth's distance from the Sun is about 1.96×10^{-7} pounds per square foot.

If the sail were oriented (slide 67) to give maximum thrust tangential to the path, then thin plastic reflectors might yield tangential thrust-weight ratio of about 2×10^{-5} (assuming a plastic thickness of 0.0005 in.). The solar sail might therefore be an interesting propulsion system for instrumented space probes. It can sail either toward or away from the Sun simply by controlling the direction of the tangential thrust component.

The greatest effectiveness of the solar sail would be for flights near the Sun. At the Venus orbital distance from the Sun, the tangential thrust to weight ratio has increased to 3.86×10^{-5}; at Mercury, the value is 1.32×10^{-4}.

Solar sails might even be useful in the Earth-satellite space region. A plastic disk, for example, might be spin-stabilized to have an orientation 45° to the Sun's rays (slide 68). The photon thrust will then always remain in the same direction. As the sail orbits through the Earth's shadow, the thrust disappears. Thus, the solar sail satellite can change its orbital path through the thrust received on the sunny side.

If one were to get enthusiastic about solar sailing, he would certainly need more information on the properties of thin plastic sheet in the radiation and high vacuum environment of space.

IX. RADIOISOTOPE SAIL

The radioisotope sail (slide 69) is perhaps useful for instrumented probes of deep space. An α emitter would be painted on one surface of a plastic membrane. The emitted α particles constitute the jet that propels this device. Ideal thrust to weight ratios of 10^{-4} might be obtainable.

Precautions would have to be taken, however, to neutralize the charge that would accumulate if electrons did not follow the α particles into space. Guidance might also be a problem.

A radioisotope photon rocket is also feasible. In this arrangement, a radioisotope-powered very hot tungsten capsule would be placed at the focal point of a thin plastic parabolic reflector. The thrust thus generated by the photon beam might propel a small payload to accelerations of perhaps 10^{-5} g.

X. ANTIGRAVITY PROPULSION

Some people have talked glibly of antigravity as a solution to space propulsion problems in the fond hope that some genius will discover the technique to accomplish this dreamed of breakthrough. If gravity could be cancelled, then an antigravity wave would presumably travel outward from the spaceship to cancel the gravitational attraction that now exists. If this hypothesized antigravity wave traveled with the speed of light, then the power requirements for propulsion would be identical to those of the photon rocket - 1330 megawatts per pound of gravity cancellation. Thus, an antigravity propulsion device would be impractical even if it were possible.

OPTIMIZATION OF SPACE PROPULSION SYSTEMS

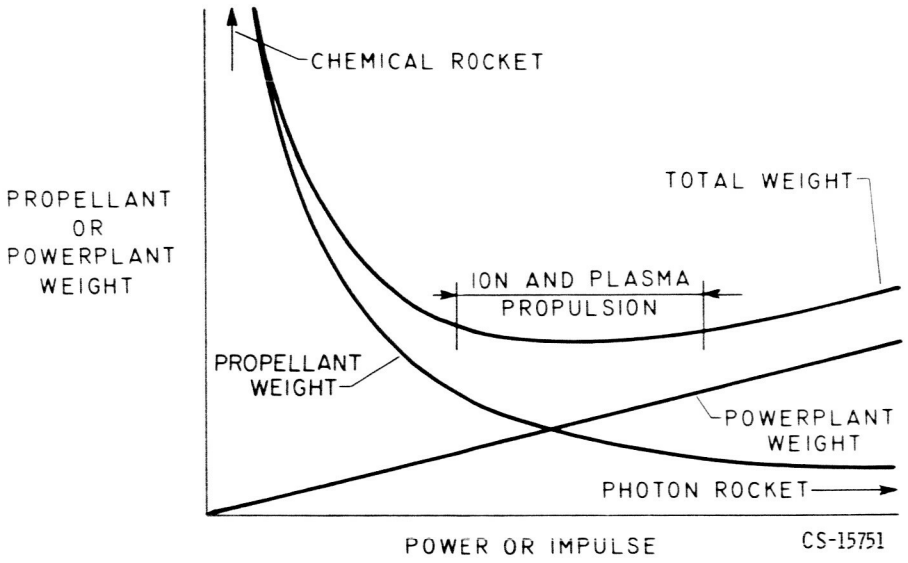

Fig. 1.

SOLID CORE HEAT TRANSFER TYPE NUCLEAR ROCKET

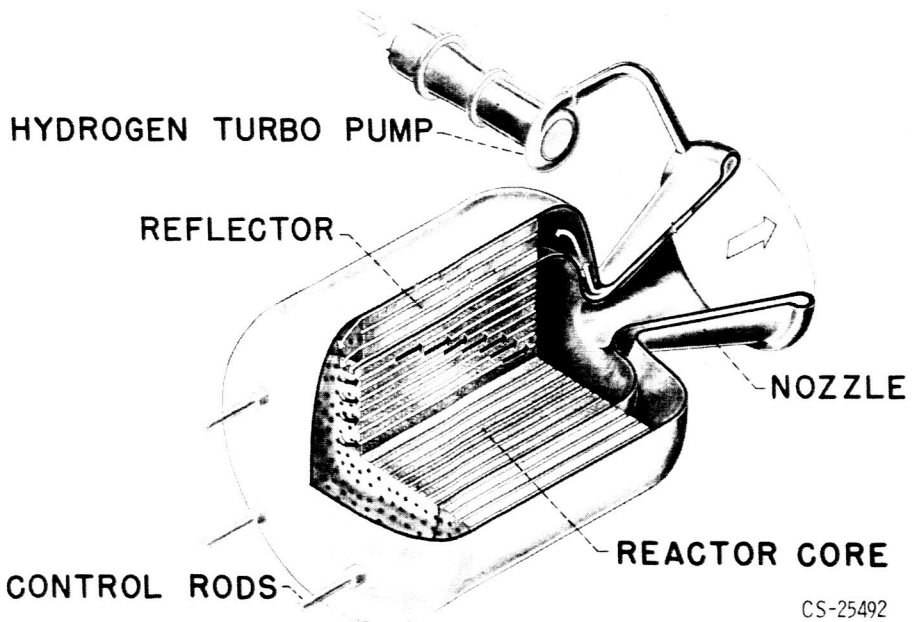

Fig. 2.

NUCLEAR ROCKET REACTORS

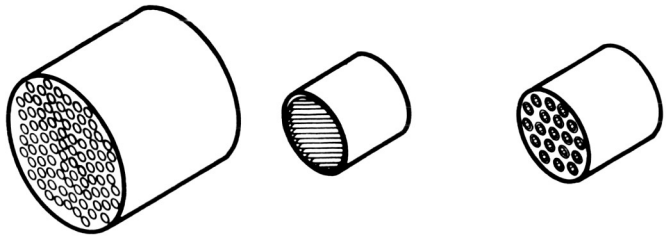

REACTOR TYPE	HOMOGENEOUS THERMAL (HOT MODERATOR)	FAST (NO MODERATOR)	HETEROGENEOUS THERMAL (COOLED MODERATOR)
MODERATING MATERIAL	GRAPHITE BERYLLIUM OXIDE	NONE	WATER HEAVY WATER BERYLLIUM BERYLLIUM OXIDE METALLIC HYDRIDES
FUEL BEARING MATERIAL	COATED GRAPHITE BERYLLIUM OXIDE	REFRACTORY METALS (W,Mo) CARBIDES (ZrC,HfC,TaC)	REFRACTORY METALS (W^{184},Mo) COATED GRAPHITE CARBIDES (ZrC)

Fig. 3. CS-25486

Fig. 4.

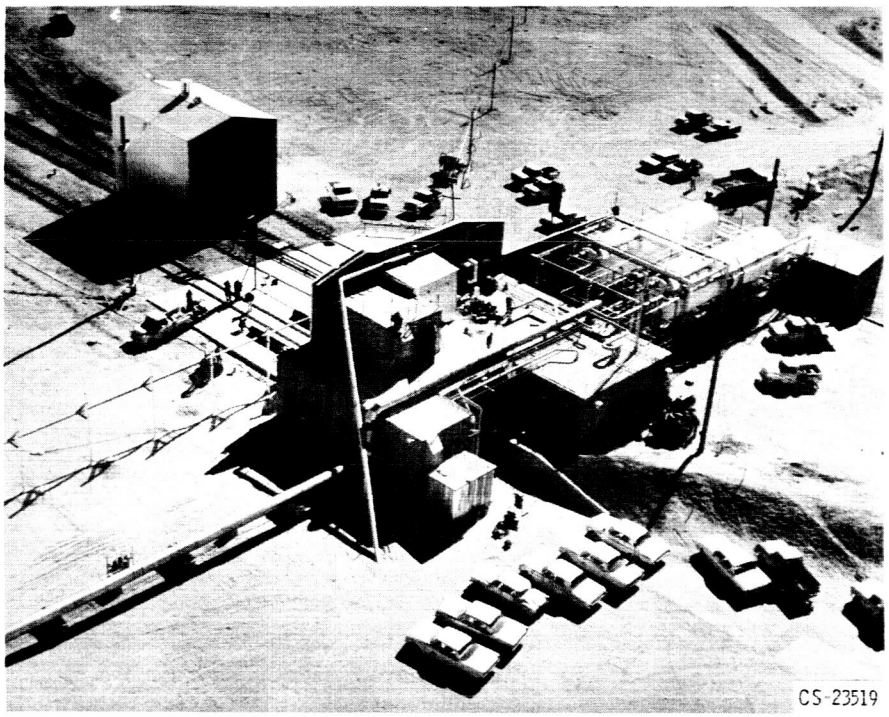

Fig. 5.

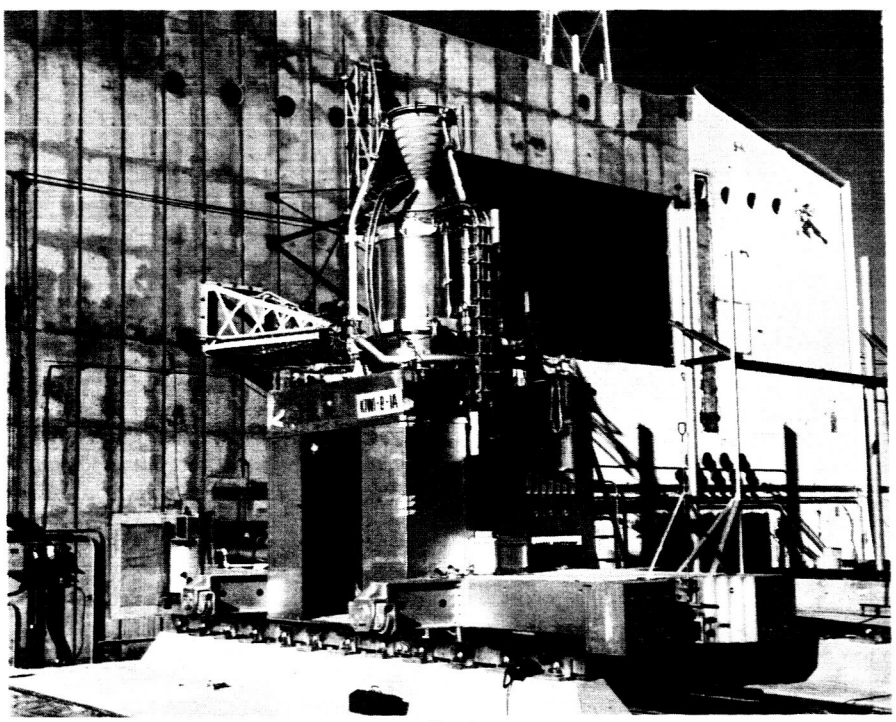

Fig. 6.

Fig. 7.

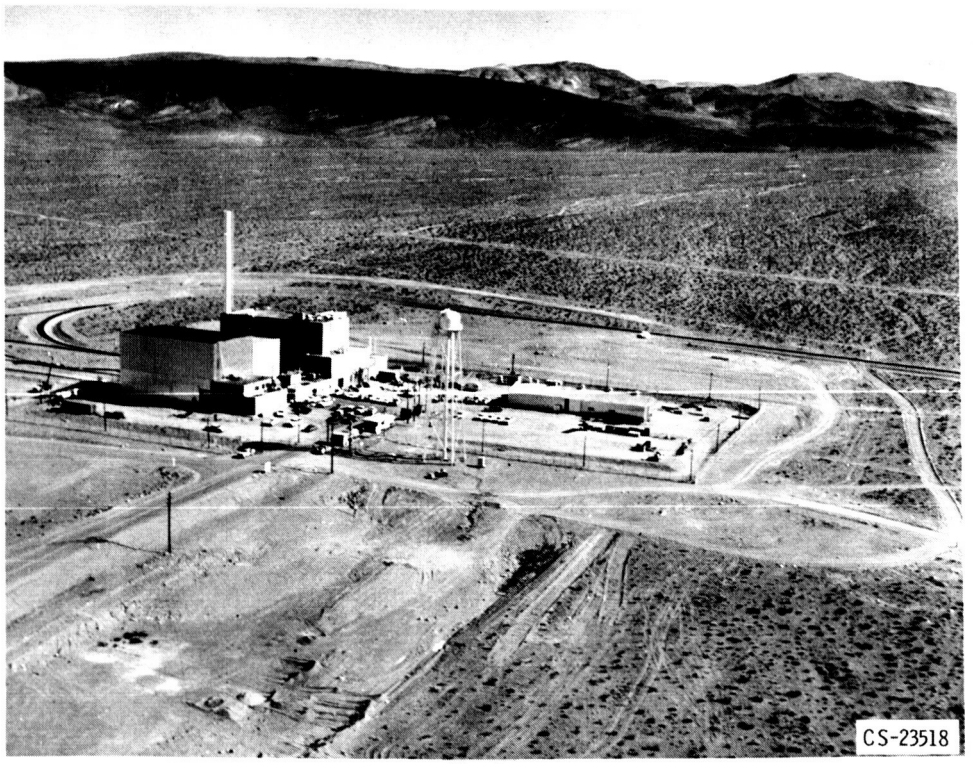

Fig. 8.

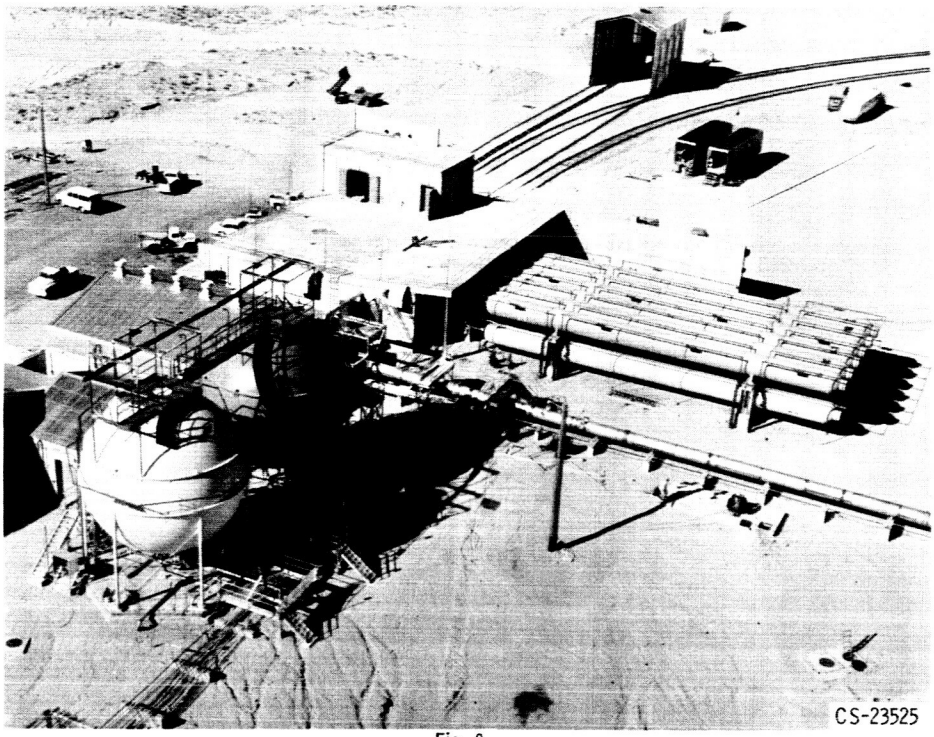

Fig. 9.

Fig. 10.

Fig. 11.

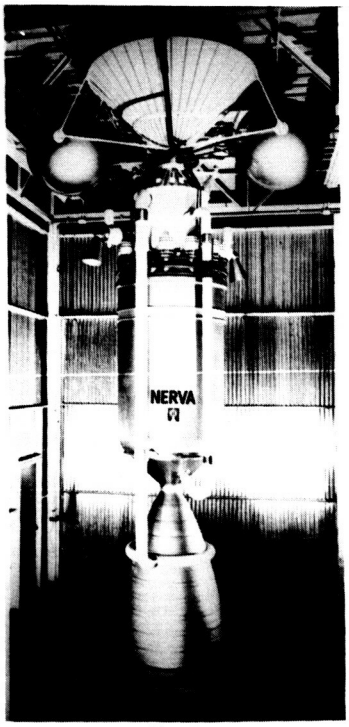

Fig. 12.

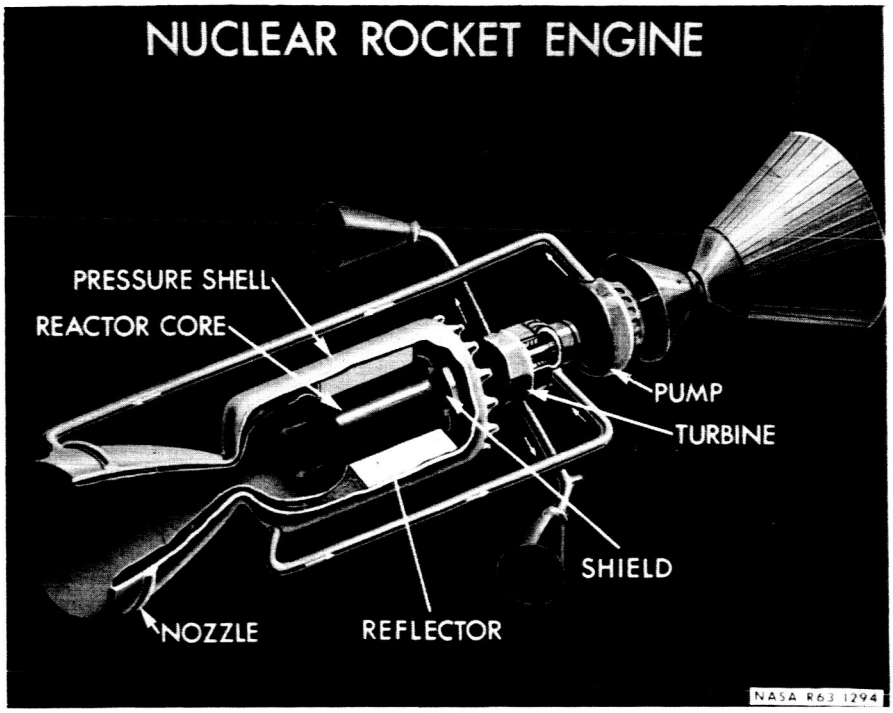
NUCLEAR ROCKET ENGINE
PRESSURE SHELL
REACTOR CORE
PUMP
TURBINE
SHIELD
NOZZLE
REFLECTOR
NASA R63 1294

Fig. 13.

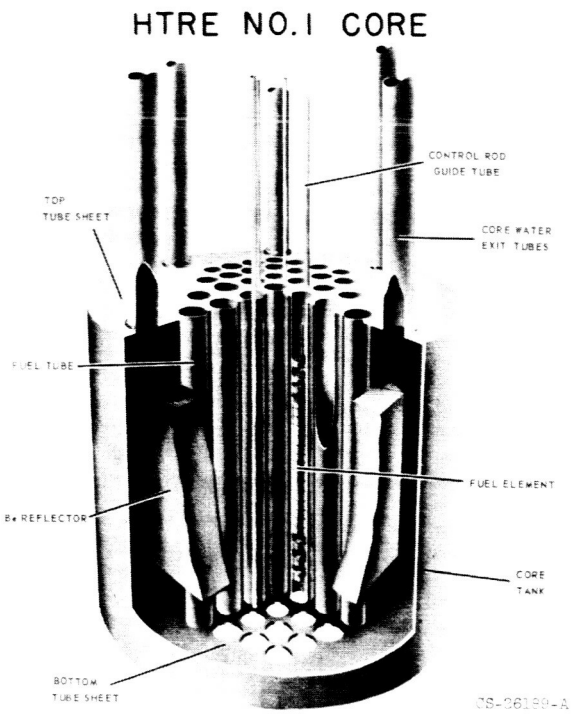
HTRE NO.1 CORE
CONTROL ROD GUIDE TUBE
TOP TUBE SHEET
CORE WATER EXIT TUBES
FUEL TUBE
FUEL ELEMENT
Be REFLECTOR
CORE TANK
BOTTOM TUBE SHEET
GS-36189-A

Fig. 14.

SCHEMATIC TUNGSTEN–WATER MODERATED REACTOR CONCEPT

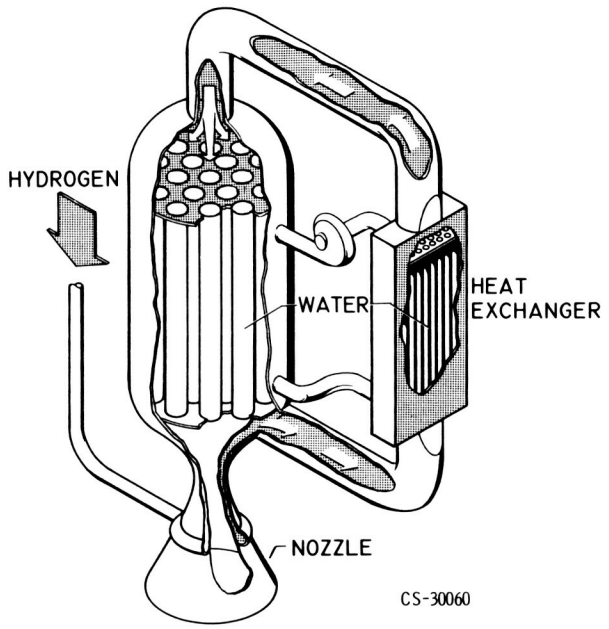

Fig. 15.

FUEL ELEMENT ASSEMBLY $W-H_2O$ REACTOR CONCEPT

$W-H_2O$ REACTER CONCEPT

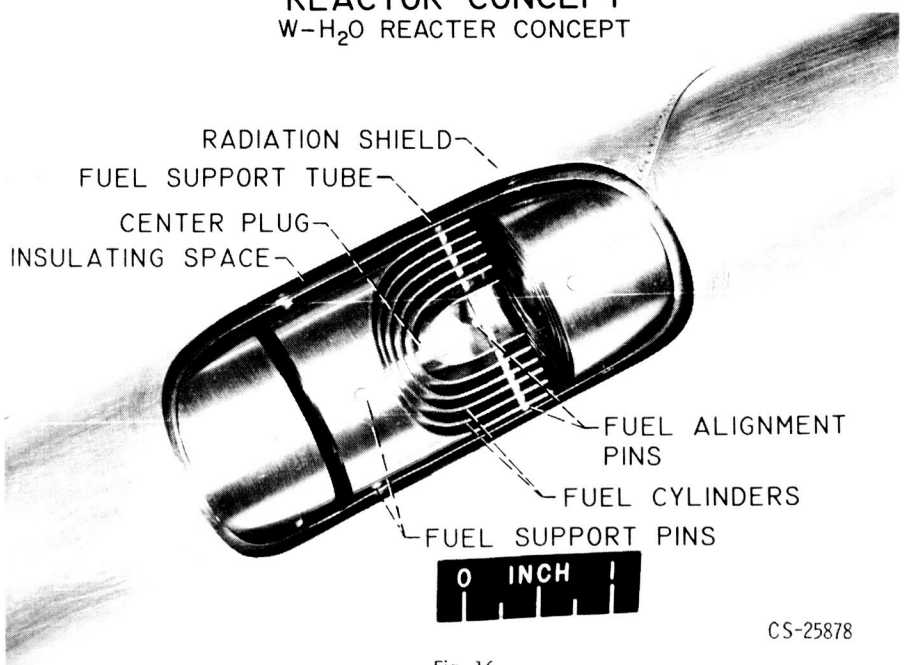

Fig. 16.

WATER MODERATED REACTOR

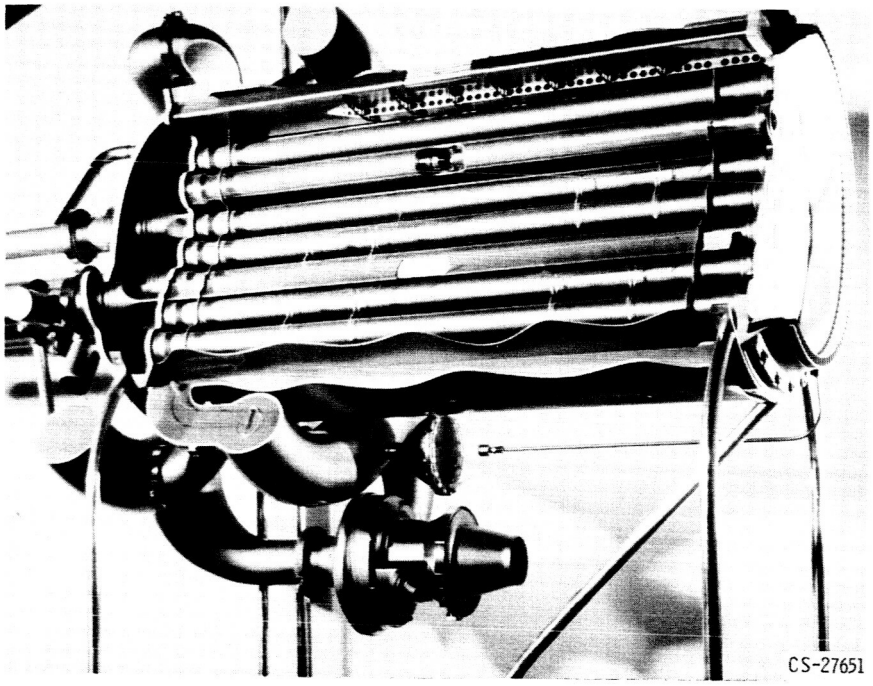

Fig. 17.

TUNGSTEN TOTAL CROSS SECTION

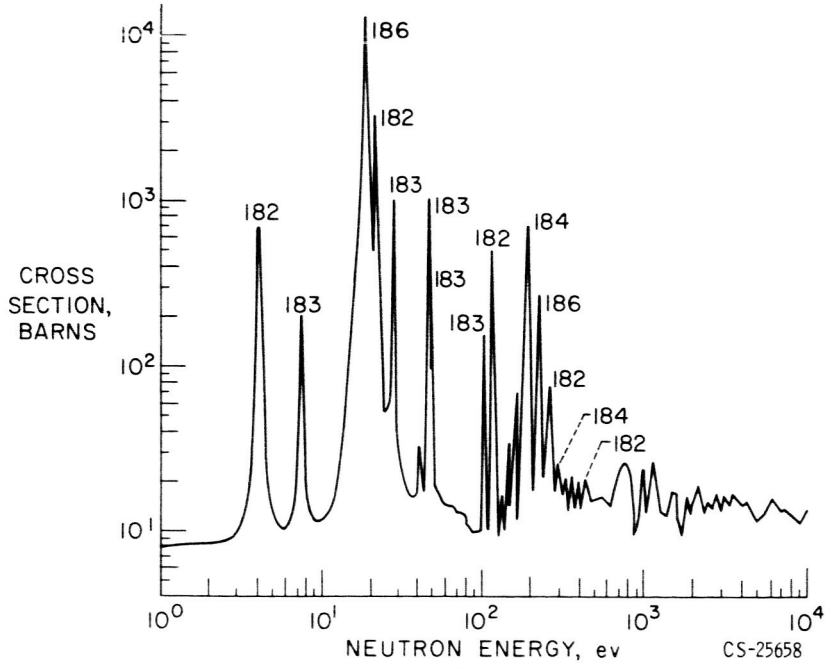

Fig. 18.

TYPICAL FUEL ELEMENT ARRAY FOR HETEROGENEOUS CORE

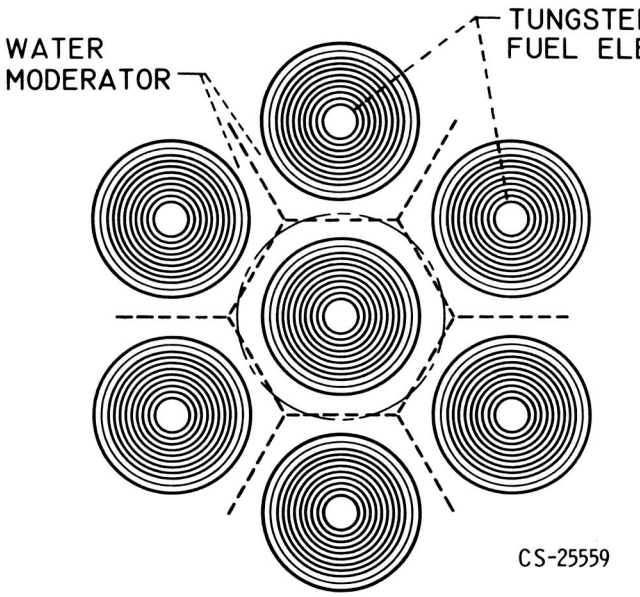

Fig. 19.

MULTIPLICATION FACTOR FOR TUNGSTEN FUEL CELL

TUNGSTEN SLABS 0.10 IN. THICK IN WATER

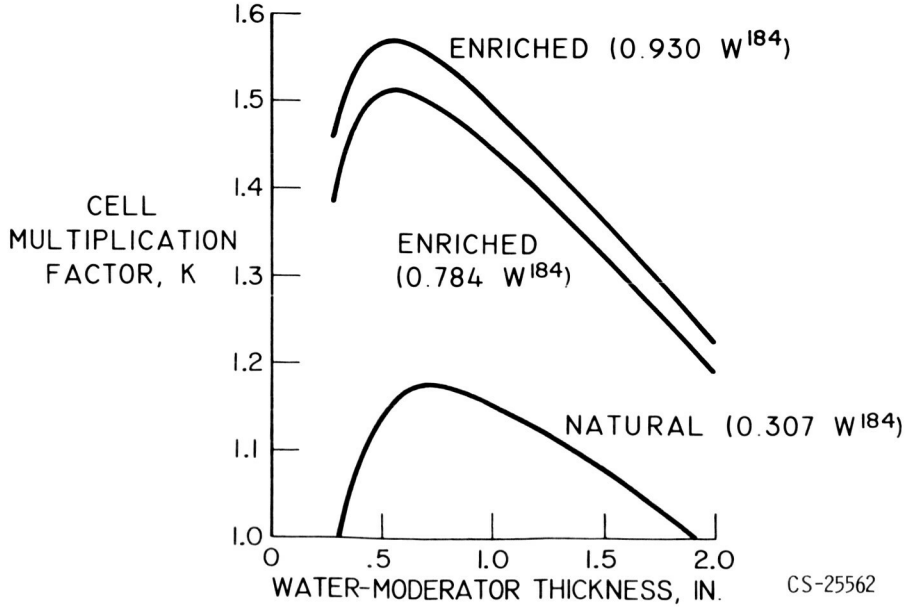

Fig. 20.

NUCLEAR ROCKET PROBE PERFORMANCE

BOOSTER, SATURN C-4

INITIAL WEIGHT IN ORBIT, 150,000 LBS

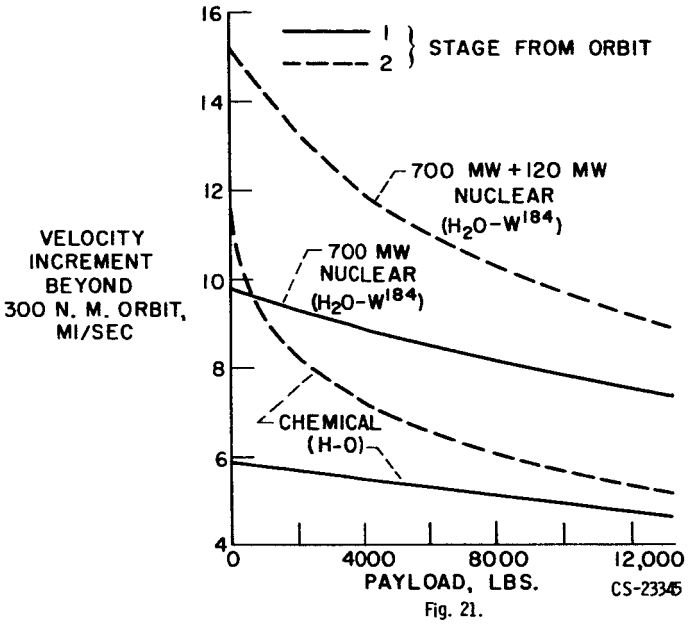

Fig. 21.

CONSTANT-THRUST TRAJECTORY FROM SATELLITE ORBIT

THRUST/WEIGHT = 10^{-4}

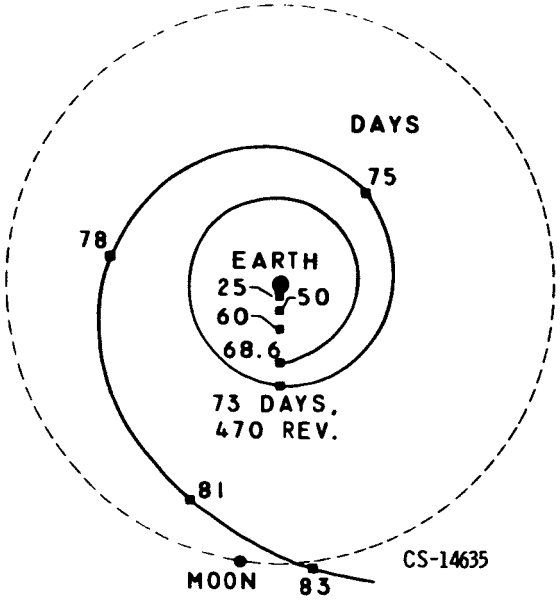

Fig. 22.

PERFORMANCE OF ELECTRIC ROCKET WITH CONSTANT PROPULSION TIME, t

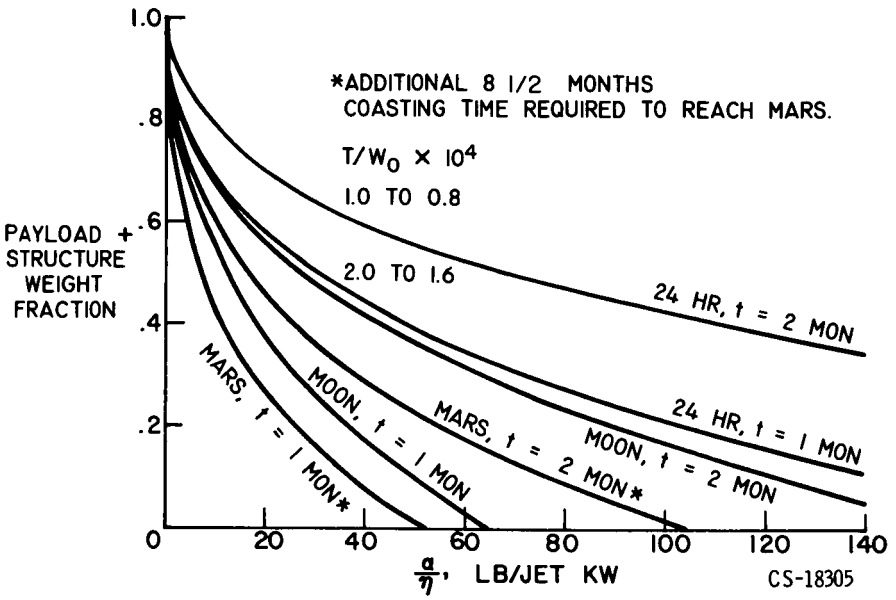

Fig. 23.

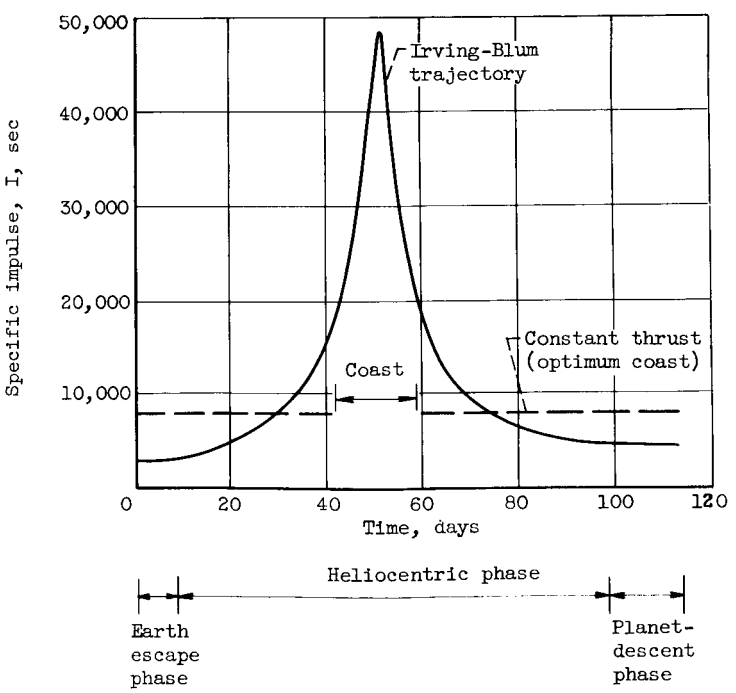

Fig. 24.

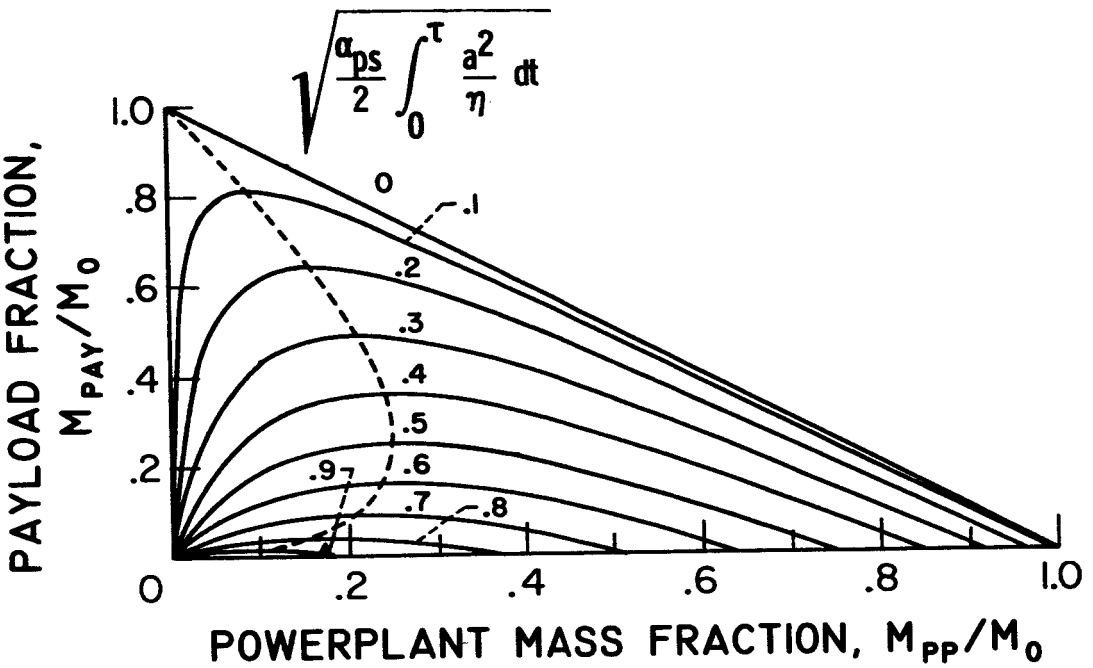

Fig. 25.

GENERAL CLASSIFICATION OF ELECTRIC ROCKET THRUSTORS

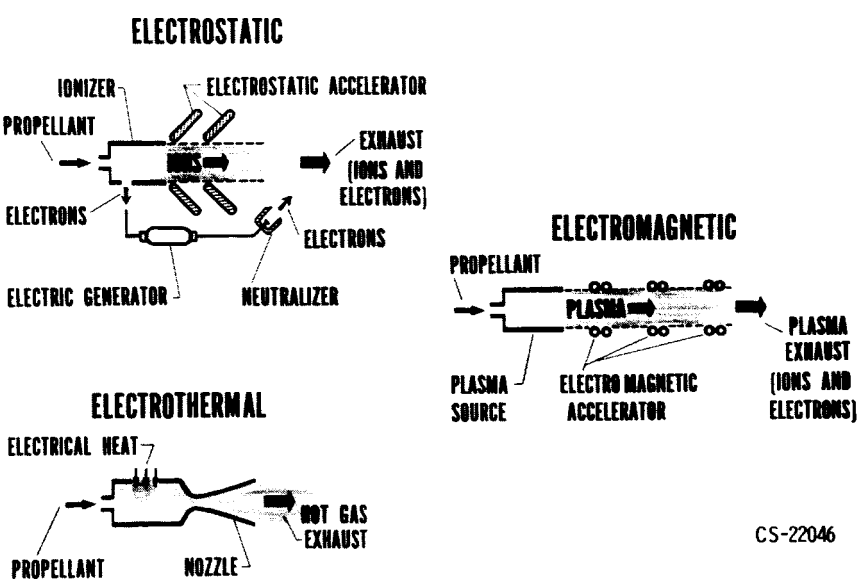

Fig. 26.

ARC-JET PROPULSION SYSTEM

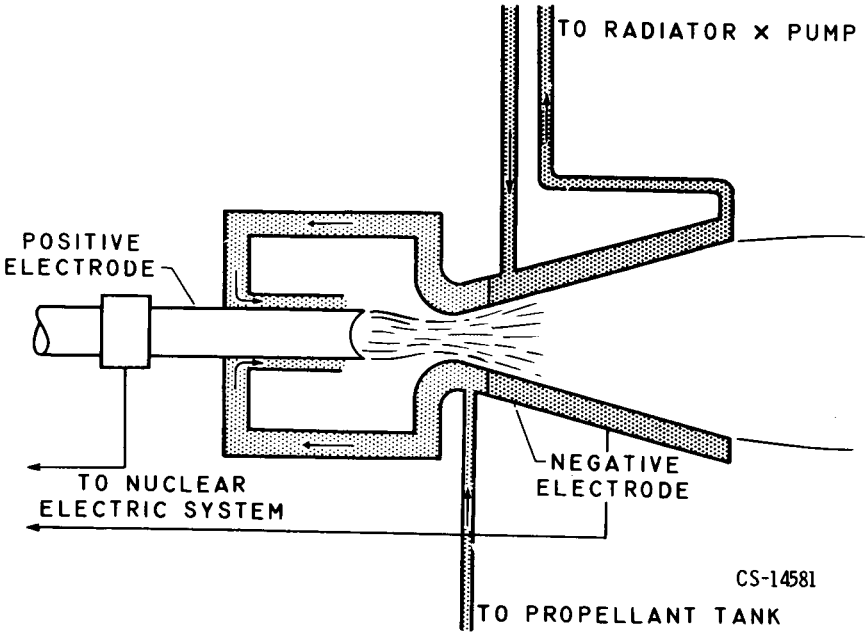

Fig. 27.

TUNGSTEN FILAMENT ELECTRO-THERMAL THRUSTOR

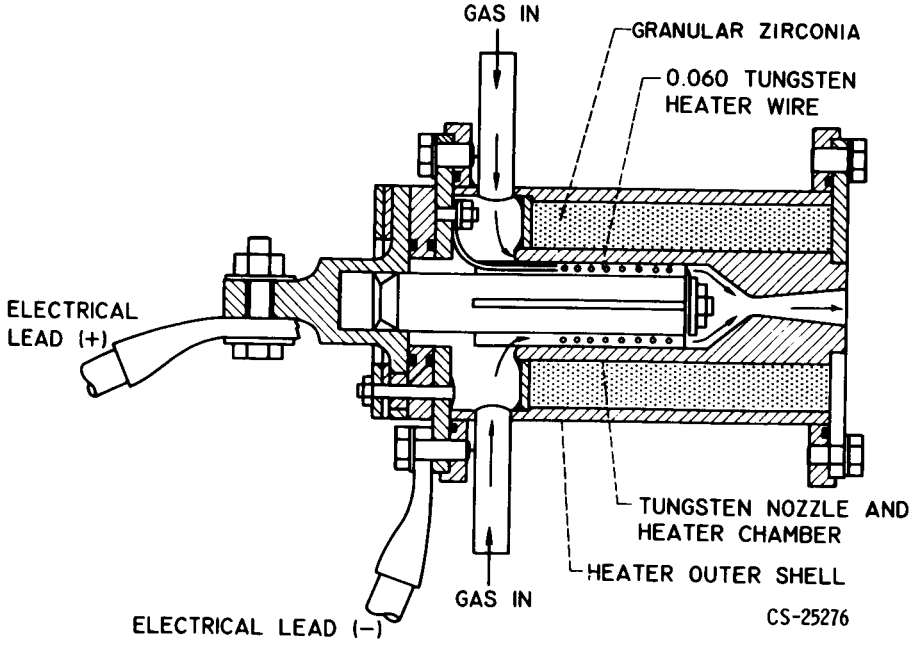

Fig. 28.

CONTACT ION ENGINE SCHEMATIC

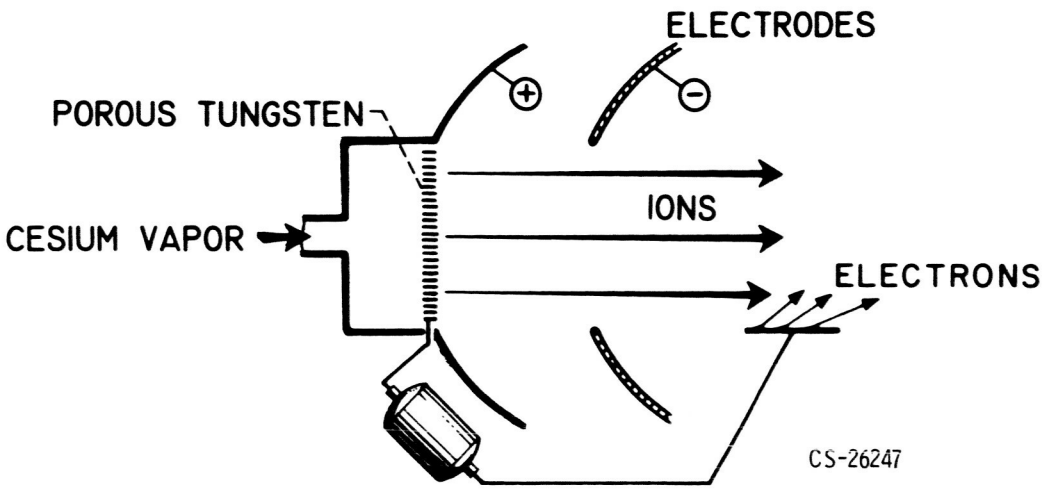

Fig. 29.

ION BEAM PHOTO

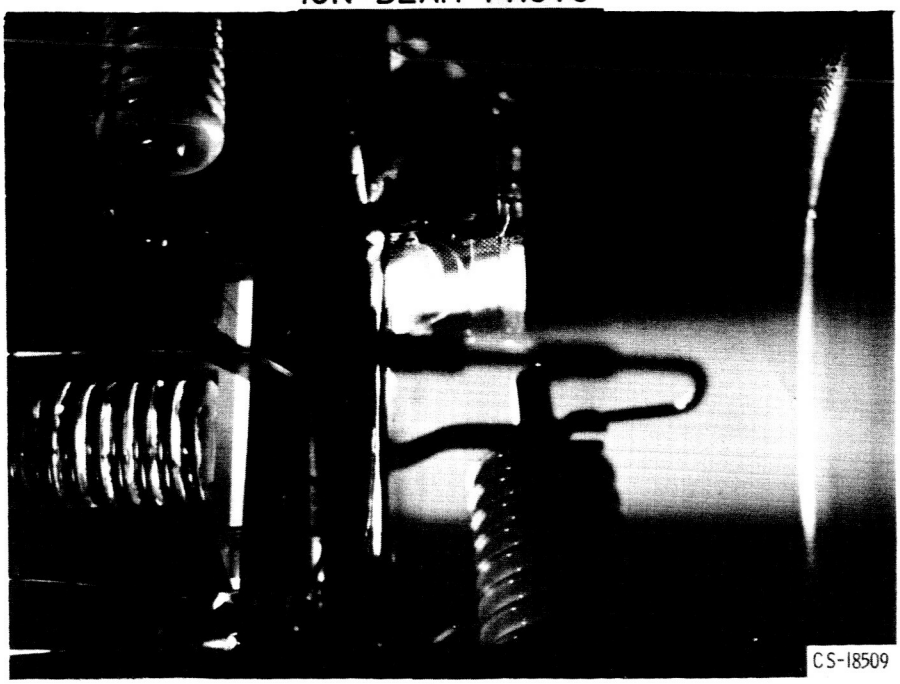

Fig. 30.

LEWIS ELECTRON-BOMBARDMENT THRUSTOR

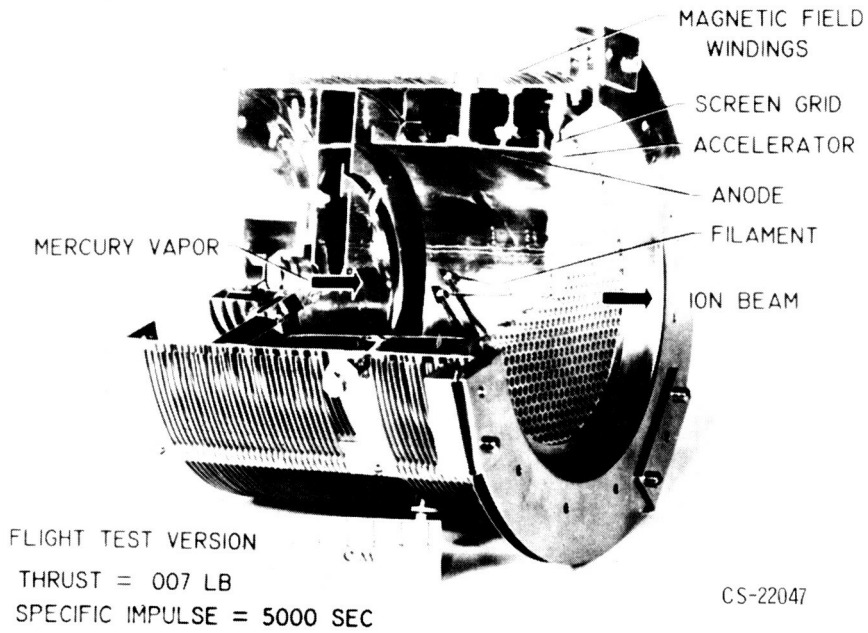

Fig. 31.

ELECTROSTATIC THRUSTOR EFFICIENCIES

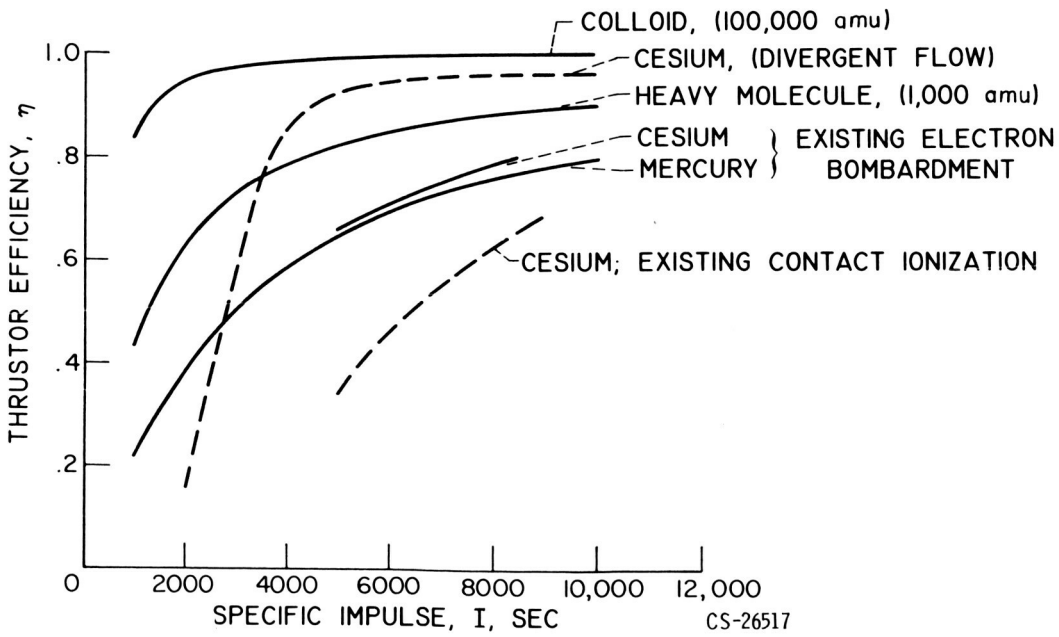

Fig. 32.

COLLOIDAL-PARTICLE THRUSTOR

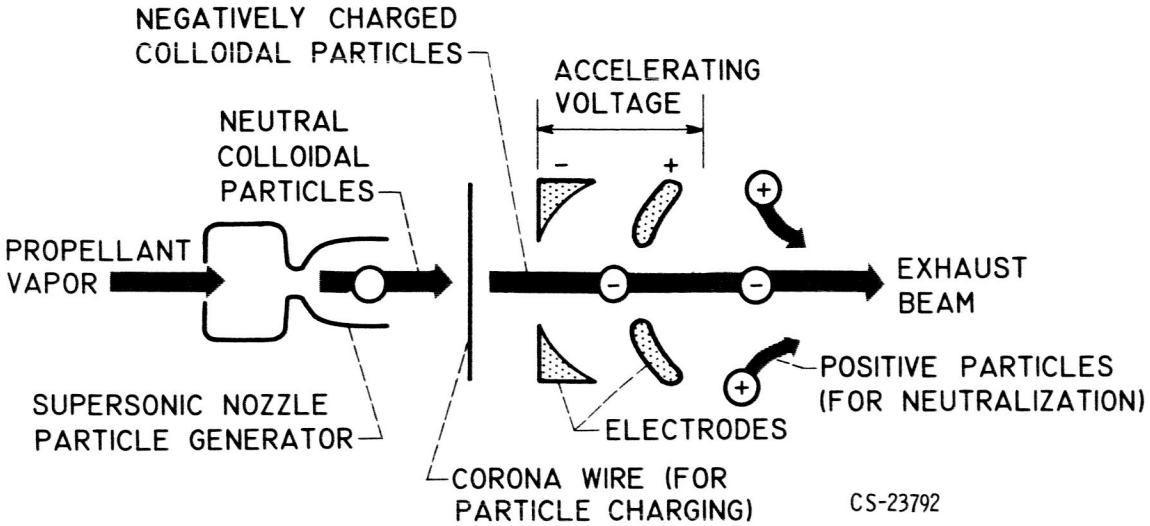

Fig. 33.

NASA LEWIS EXPERIMENTAL
COLLOIDAL–PARTICLE THRUSTOR
CORONA–DISCHARGE CHARGING

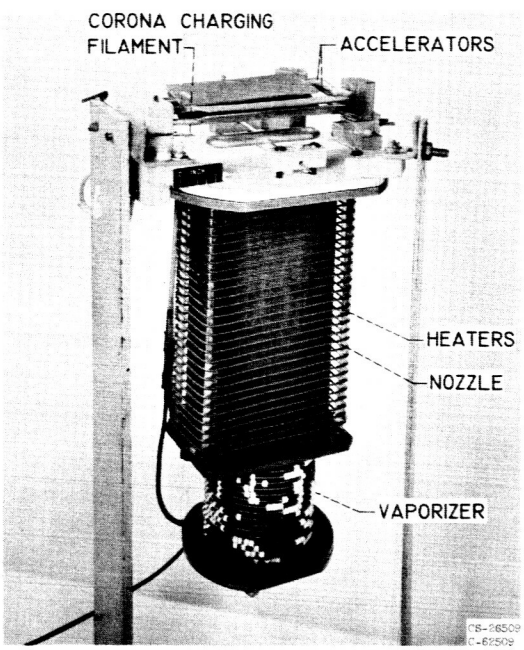

Fig. 34.

NASA LEWIS EXPERIMENTAL COLLOIDAL–PARTICLE THRUSTOR

ELECTRON–BOMBARDMENT CHARGING CHAMBER

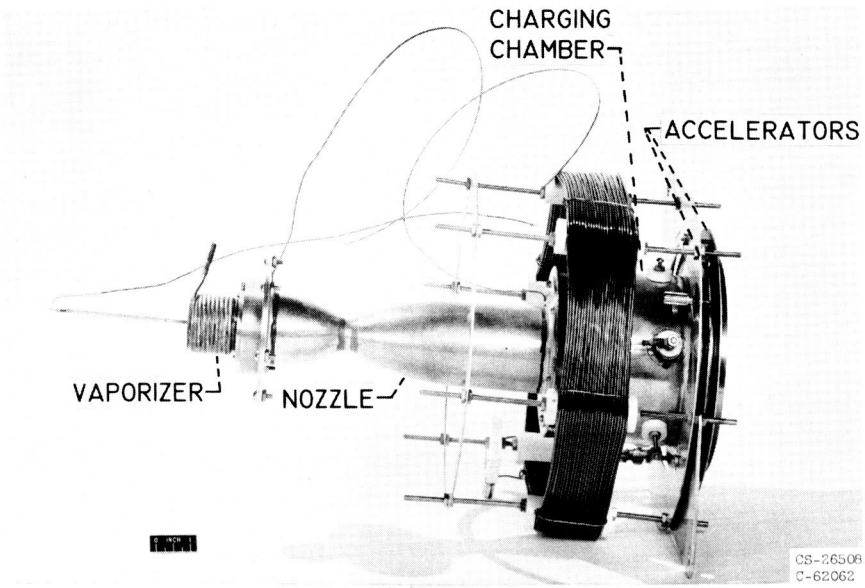

Fig. 35.

VON ARDENNE ION ROCKET

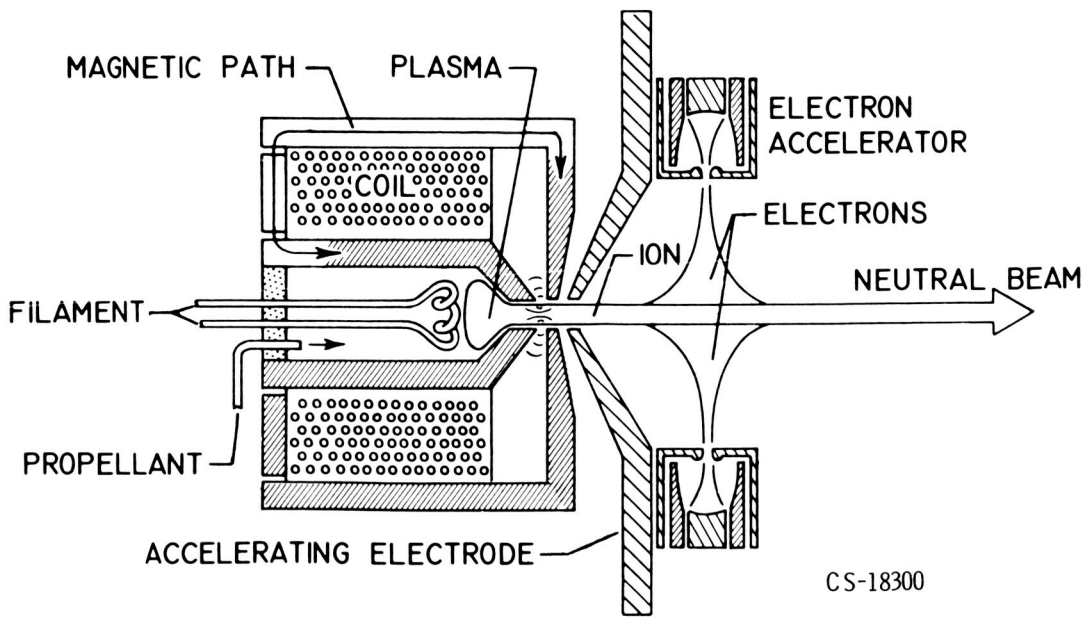

Fig. 36.

HALL CURRENT ION ACCELERATOR

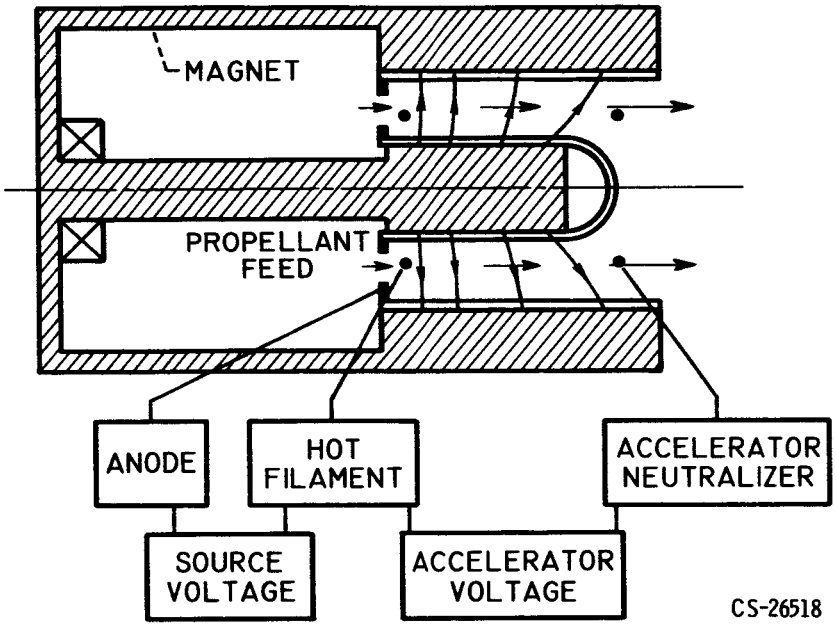

Fig. 37.

CHARGED PARTICLE MOTIONS IN MAGNETIC AND ELECTRIC FIELDS

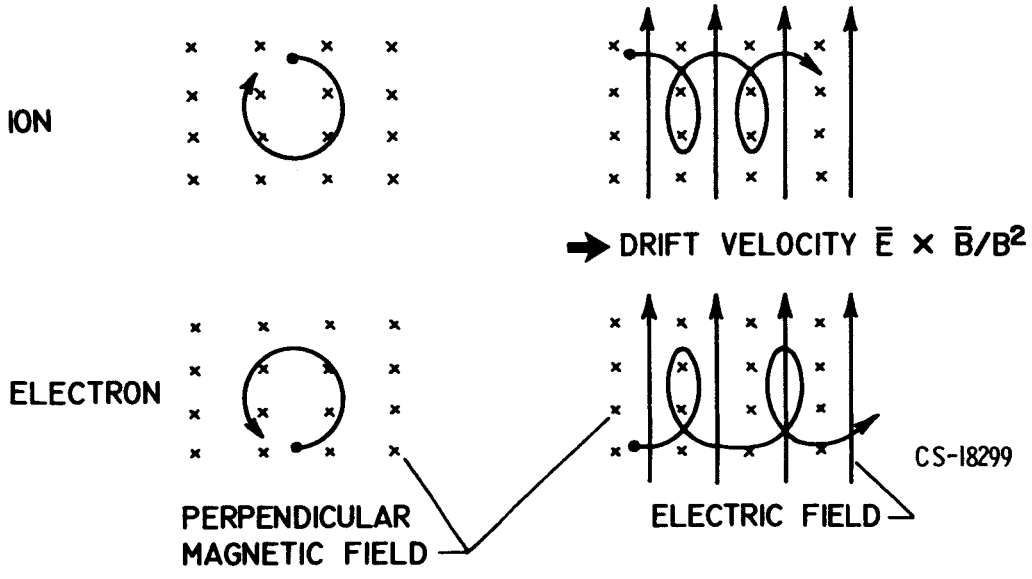

Fig. 38.

E X B ACCELERATOR

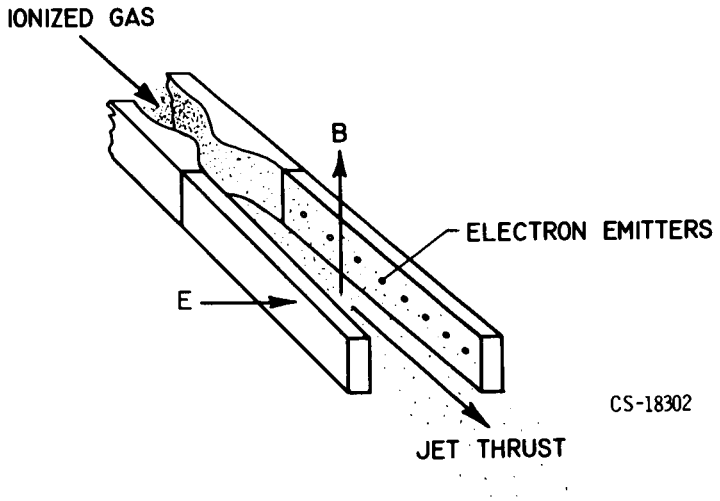

Fig. 39.

COAXIAL PLASMA GUN

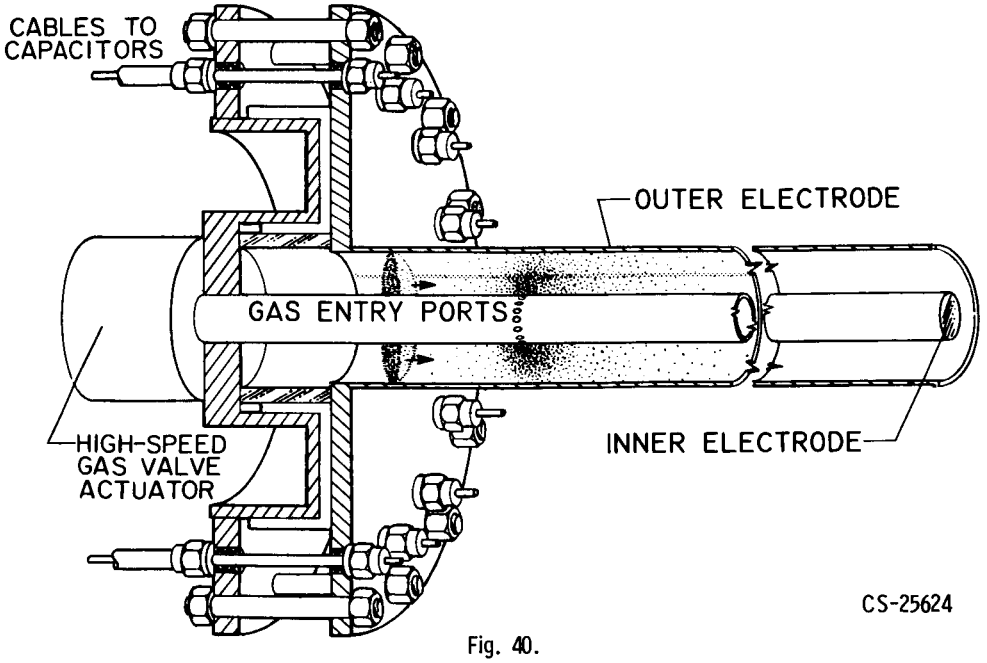

Fig. 40.

PLASMA PROJECTION VIA THE PINCH EFFECT

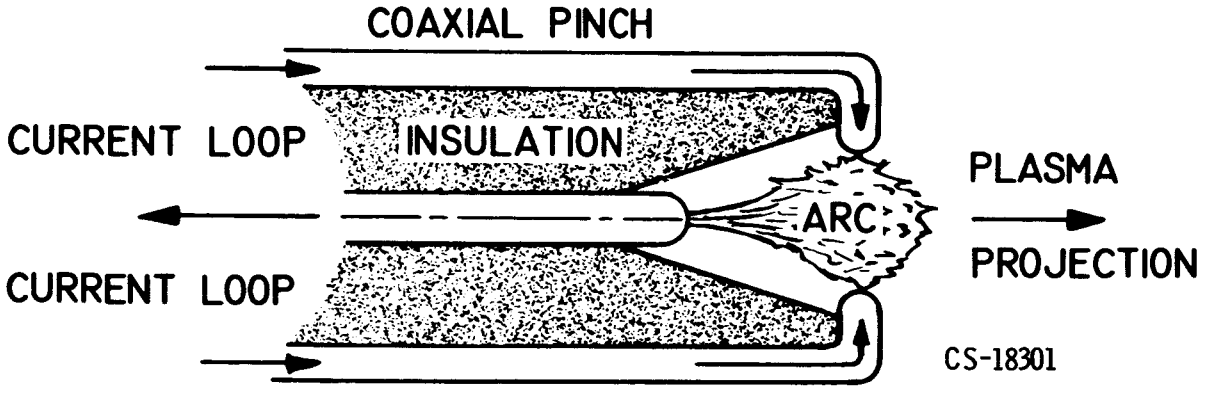

Fig. 41.

MAGNETIC MIRROR PLASMA ROCKET

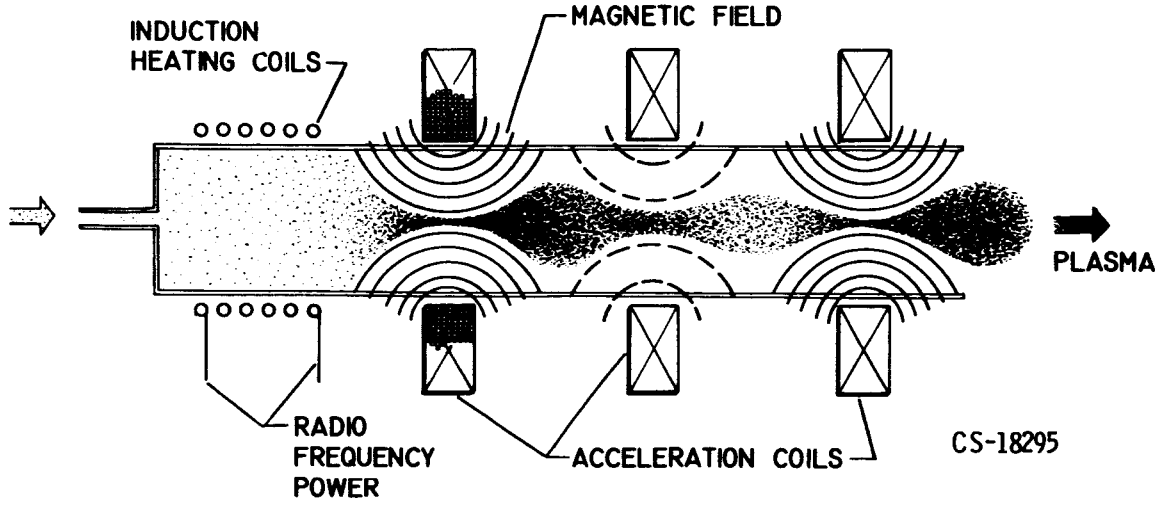

Fig. 42.

MANNED MARS MISSION

CREW SHIELDING FOR 100 REM DOSE, METEOROID SHIELDING FOR P_o = 0.999

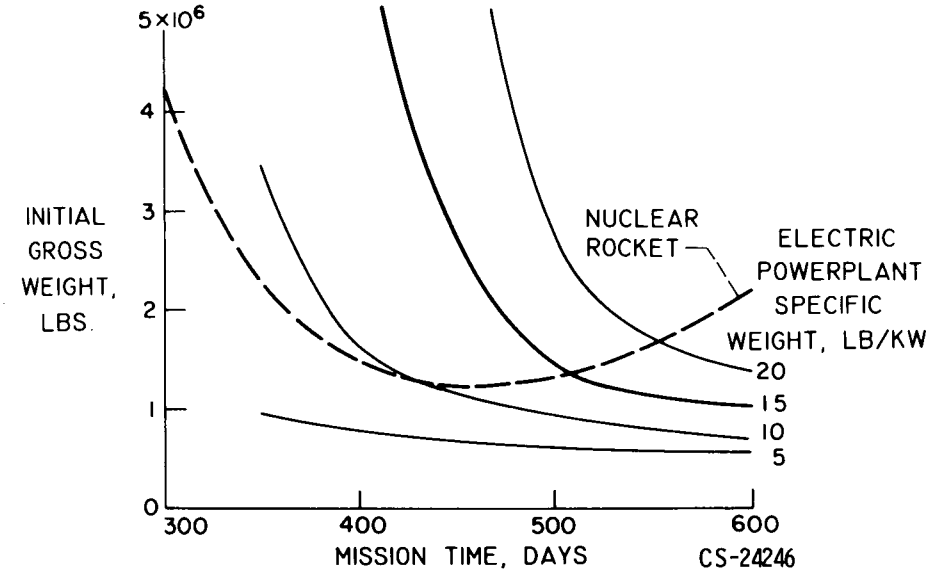

Fig. 43.

WEIGHT GROWTH DUE TO INEFFICIENCIES

[GENERATOR AND POWER CONDITIONING OPERATE AT 700° F; SPECIFIC IMPULSE OF EXISTING THRUSTOR, 9000 SEC.]

COMPONENT	EFFICIENCY	SPECIFIC WEIGHT, LB/KW	EFFECTIVE SPECIFIC WEIGHT, LB/KW
POWERPLANT	----	22.0	22.0
GENERATOR	0.92	1.0	2.9
POWER CONDITIONING	.91	2.1	4.6
THRUSTOR	.88	1	----
CONSTANT SPECIFIC IMPULSE	----	5.3	----
THRUSTOR SYSTEM	----	----	10.5
TOTAL			40.0

CS-34594

Fig. 44.

E-2253-I

ELECTRIC ROCKET AND NUCLEAR ROCKET EQUAL PAYLOAD WEIGHT

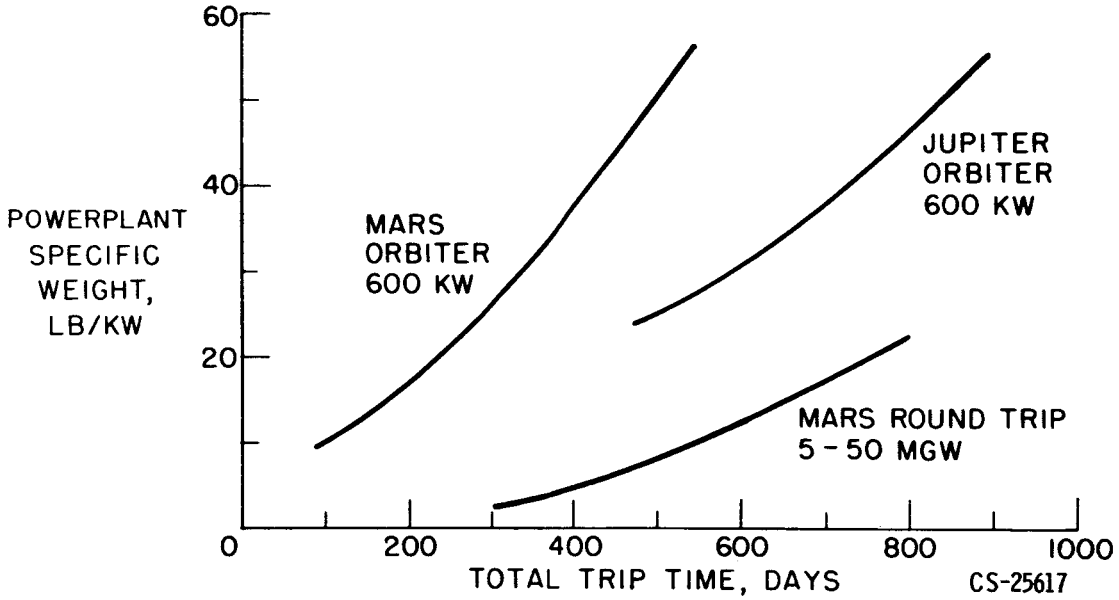

Fig. 45.

COMPARISON OF ALL–ELECTRIC, ALL–NUCLEAR, AND COMBINED ROCKET SYSTEMS

SEVEN-MAN MARS MISSION; WAIT TIME, 40 DAYS; SPECIFIC POWERPLANT MASS, 15.4 LB/KW; ENTRY VELOCITY, 52,000 FT/SEC

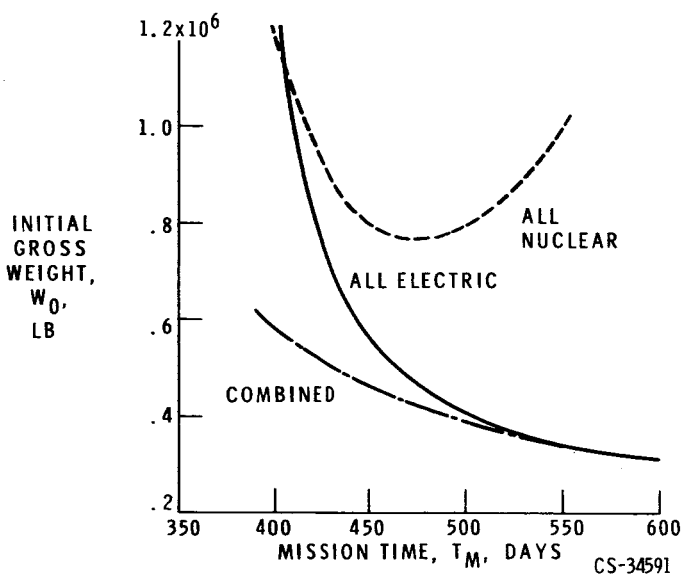

Fig. 46.

EFFECT OF COMBINED ROCKET ON ALLOWED POWERPLANT SPECIFIC WEIGHT

MARS ROUND TRIP; APPROACH SPEED AT EARTH, 37,000 FT/SEC

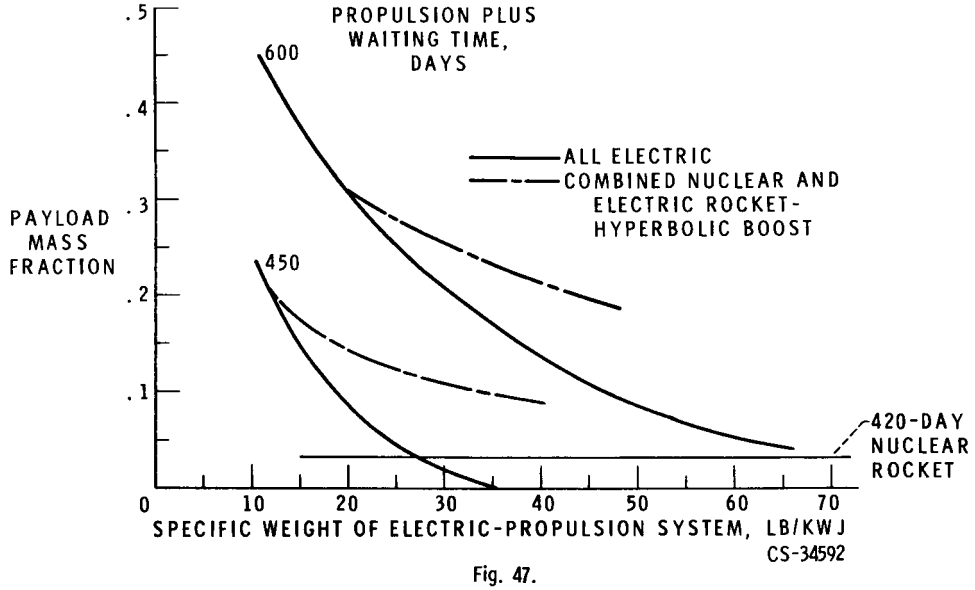

Fig. 47.

SCHEMATIC OF RANKINE CYCLE
SPACE POWER SYSTEM

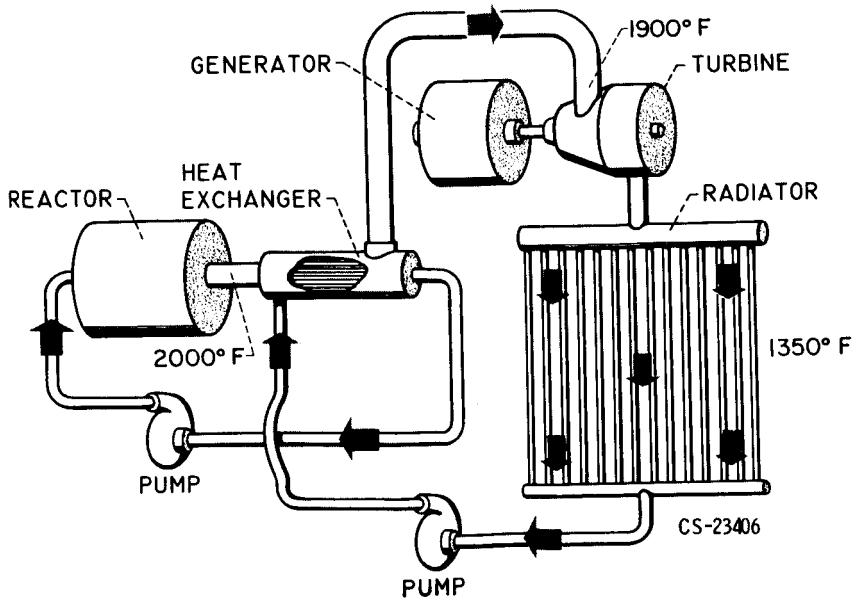

Fig. 48.

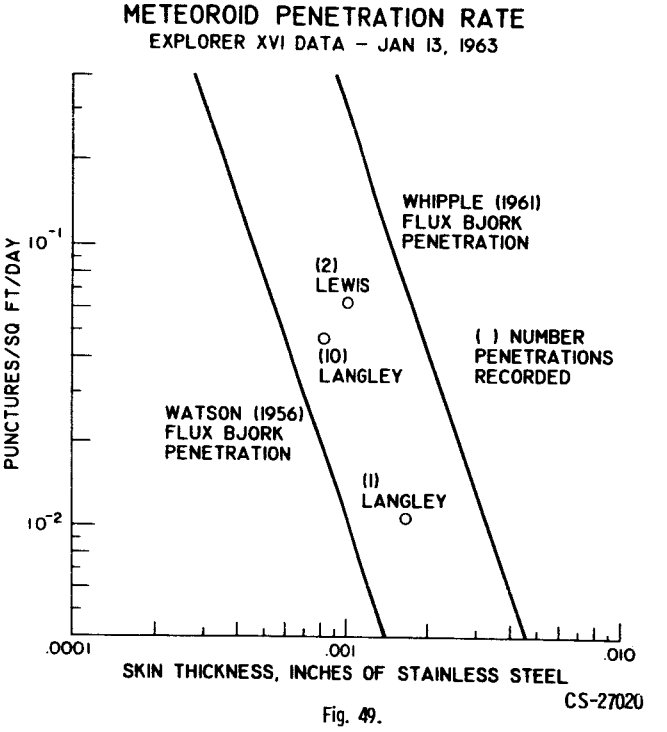

Fig. 49.

EFFECT OF SEGMENTING ON RADIATOR PANEL WEIGHT

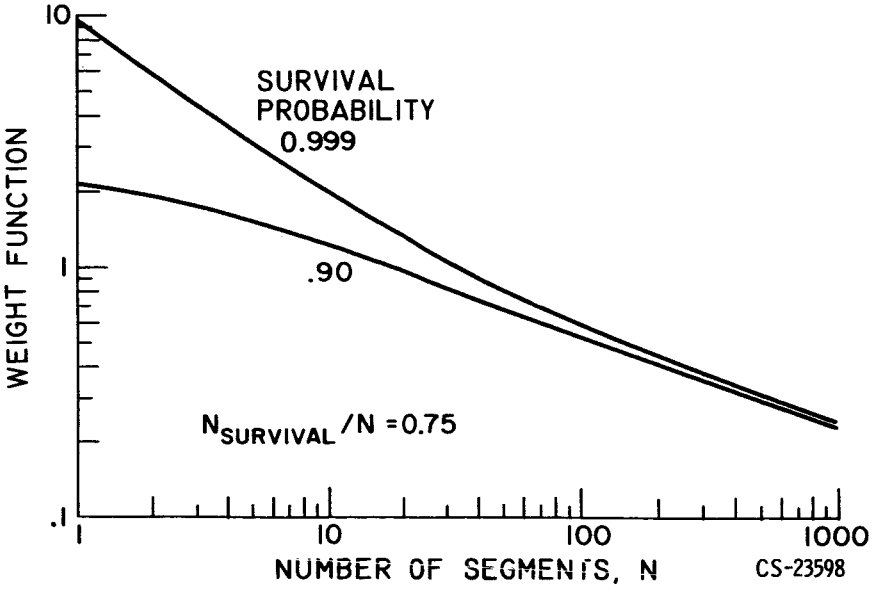

Fig. 50

NON-FLUID RADIATORS

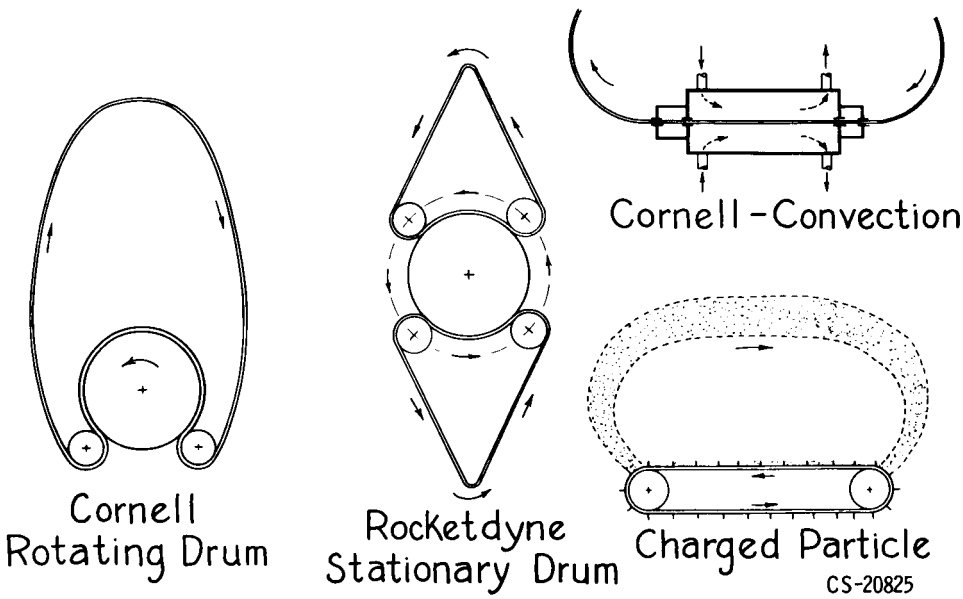

Fig. 51.

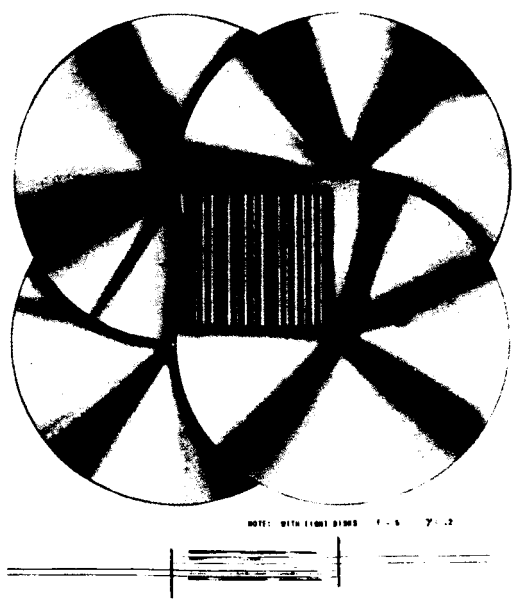

CONFIGURATION FOR FOUR OR EIGHT DISK RADIATION AMPLIFIER (FOUR ILLUSTRATED)

Ref: Weatherston, R.C.: IAS Paper No. 62-73, Jan. 1962 (Cornell Aeronautical Laboratory, Inc.

Fig. 52.

EFFECT OF TURBINE INLET TEMPERATURE ON RADIATOR AREA

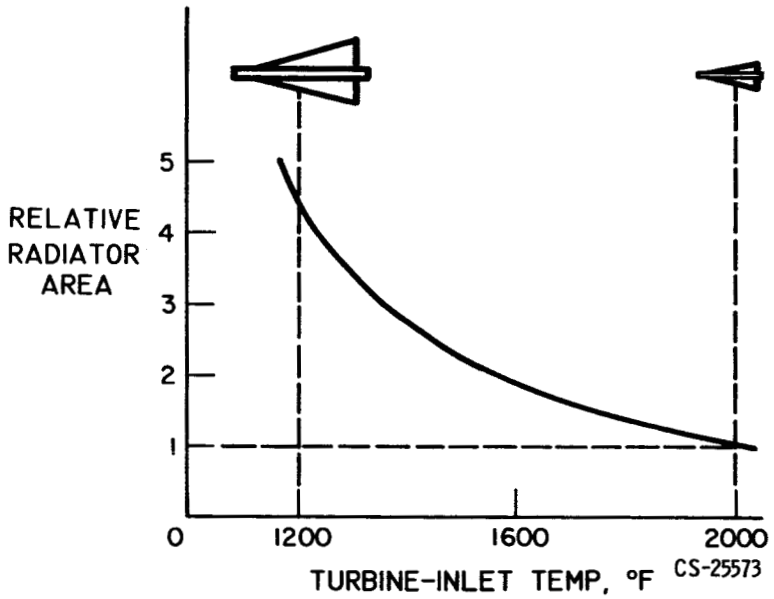

Fig. 53.

EFFECT OF TURBINE EFFICIENCY ON RADIATOR AREA

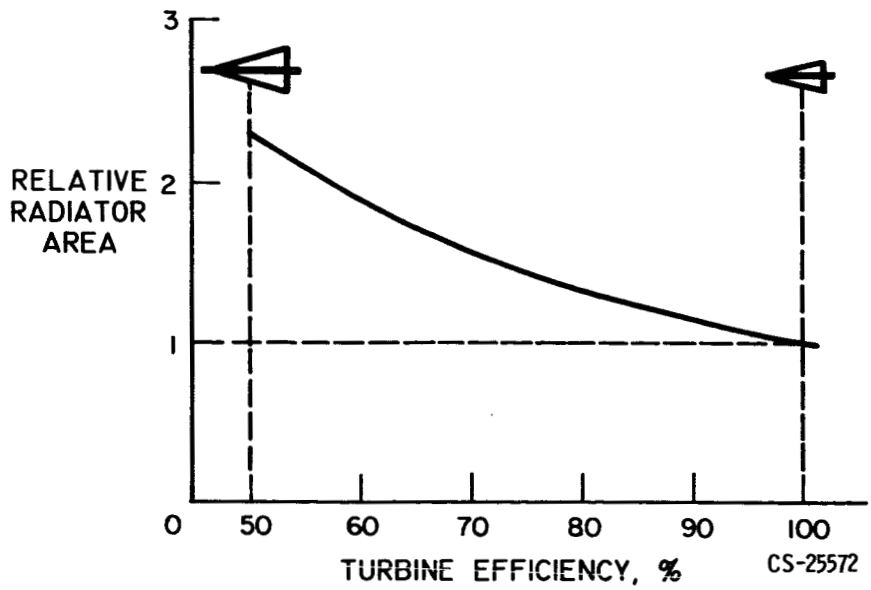

Fig. 54.

EFFECT OF SUPERHEAT ON RADIATOR AREA

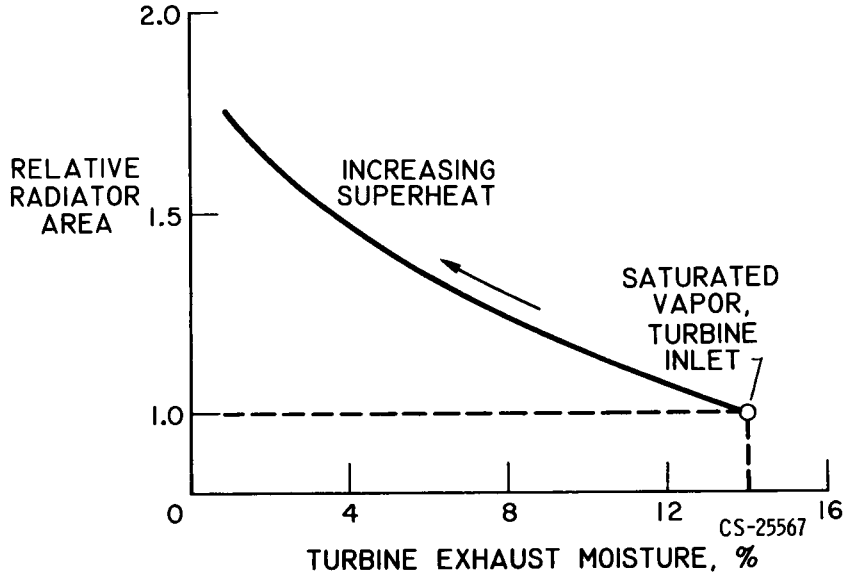

Fig. 55.

SCHEMATIC OF BRAYTON CYCLE SPACE POWER SYSTEM

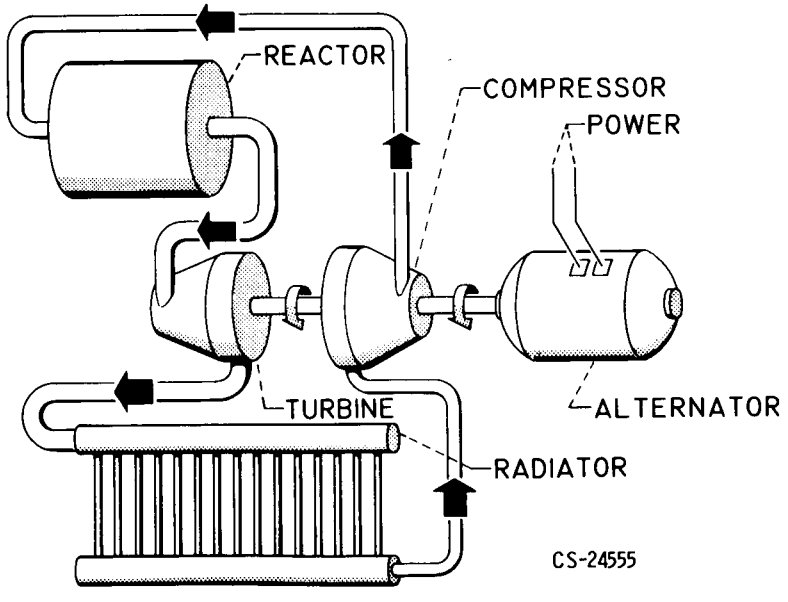

Fig. 56.

THERMIONIC CONVERTER

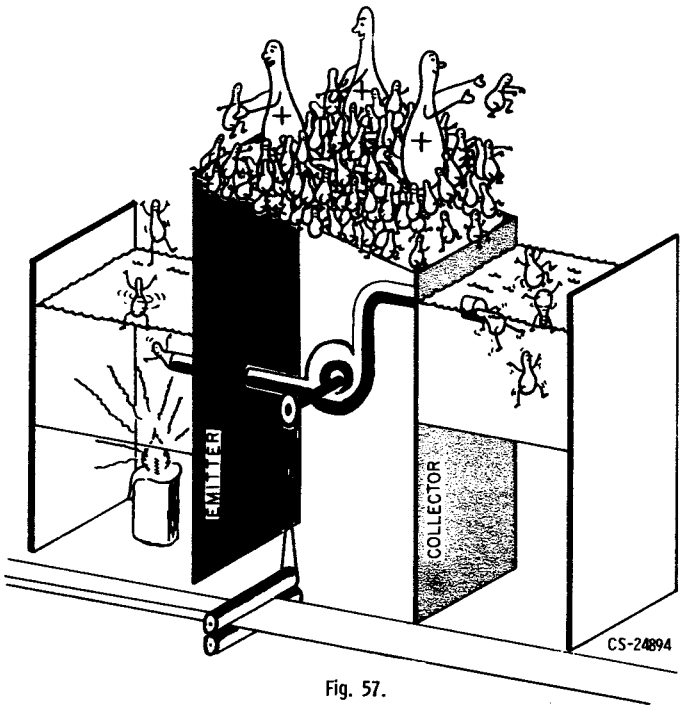

Fig. 57.

NUCLEAR THERMIONIC POWER SYSTEM

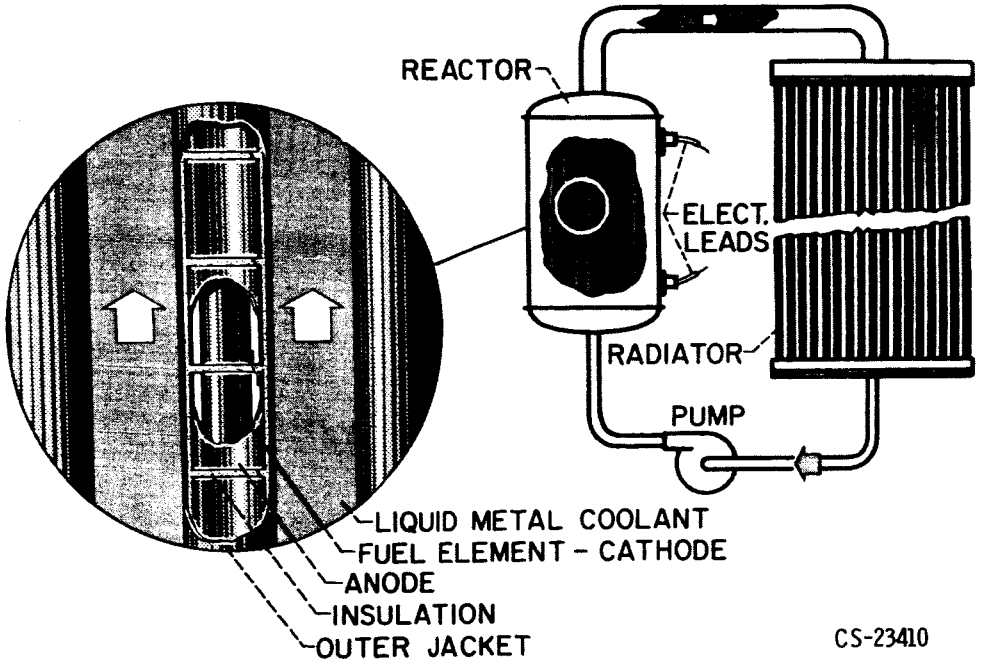

Fig. 58.

GASEOUS CAVITY REACTOR

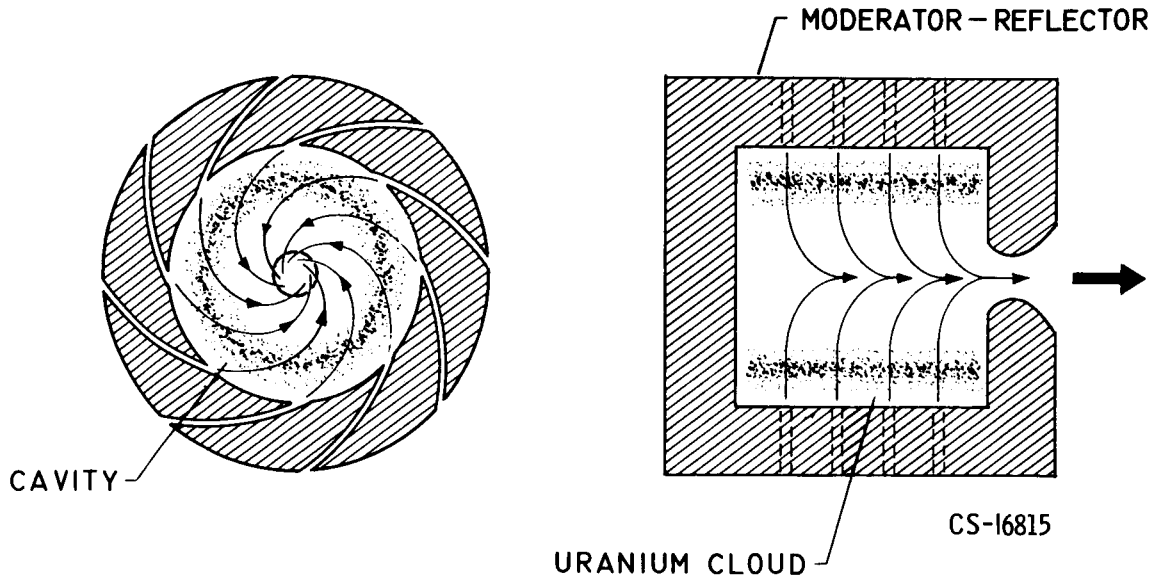

Fig. 59.

VORTEX GAS CORE REACTOR

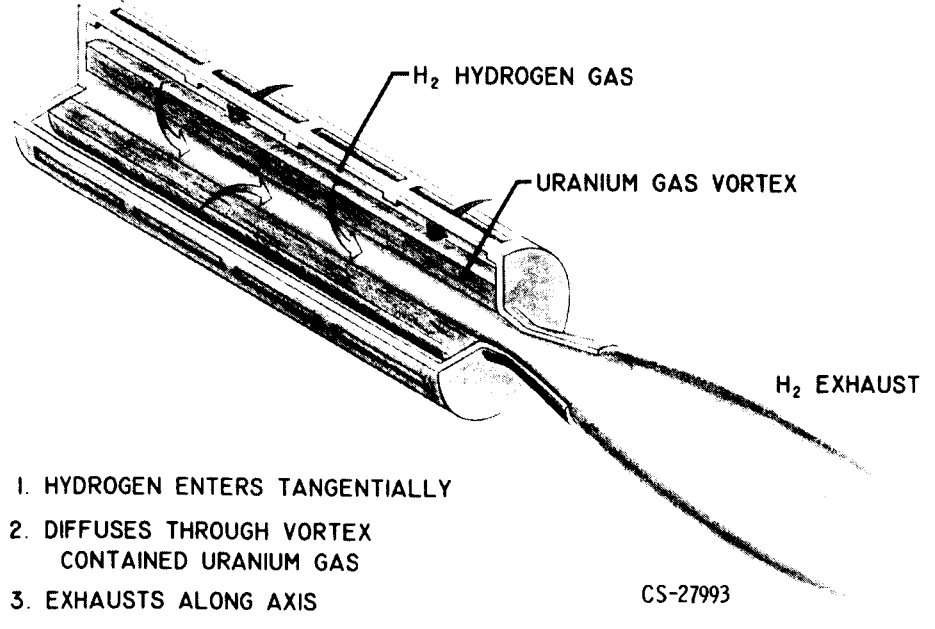

Fig. 60.

VORTEX TUBE AND VORTEX MATRICES

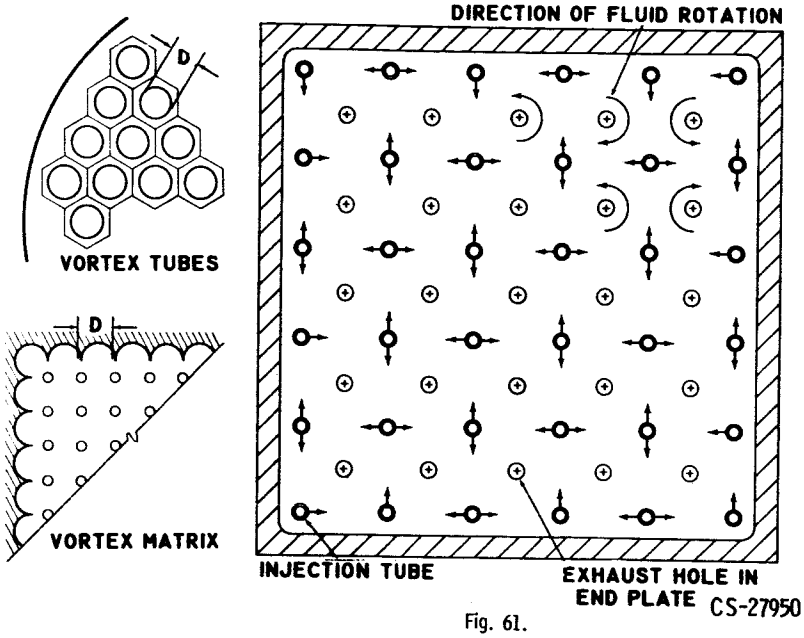

Fig. 61.

COAXIAL JET REACTOR

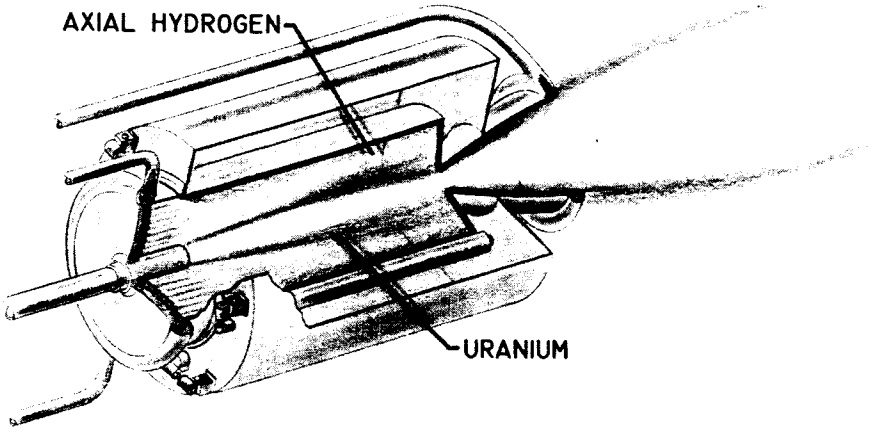

1. URANIUM AND HYDROGEN FLOW AXIALLY
2. URANIUM FLOWS MUCH SLOWER THAN HYDROGEN
3. TURBULENT MIXING GRADUALLY CONSUMES URANIUM CS-27997
4. LOW SPEED HYDROGEN BUFFER LAYER MINIMIZES URANIUM LOSS

Fig. 62.

WHEEL FLOW REACTOR

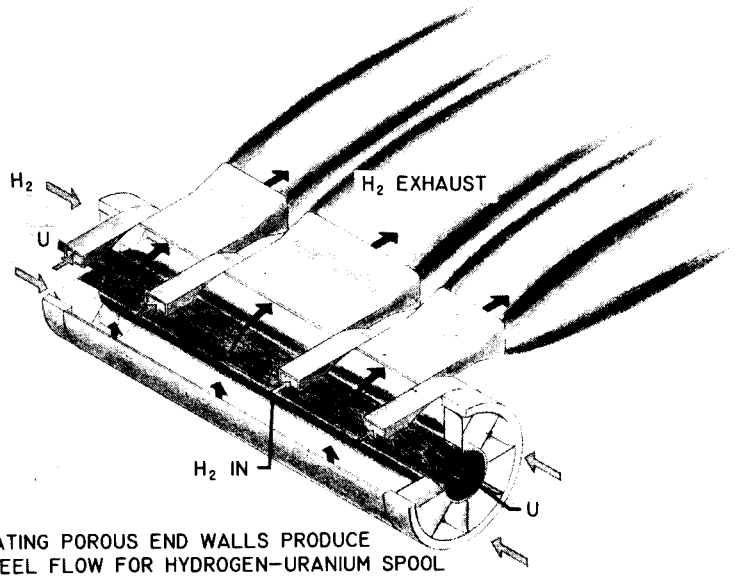

1. ROTATING POROUS END WALLS PRODUCE WHEEL FLOW FOR HYDROGEN–URANIUM SPOOL
2. AXIAL VELOCITIES TAILORED TO GIVE MINIMUM SHEAR
3. PRINCIPAL HYDROGEN FLOW ENTERS AND LEAVES TANGENTIALLY

CS-27996

Fig. 63.

FUSION REACTIONS

$$D + D \longrightarrow He^3\ (0.8\ MEV) + n\ (2.4\ MEV)$$

$$D + D \longrightarrow T\ (1.0\ MEV) + p\ (3.0\ MEV)$$

$$D + T \longrightarrow He^4\ (3.5\ MEV) + n\ (14.1\ MEV)$$

$$D + He^3 \longrightarrow He^4\ (3.6\ MEV) + p\ (14.7\ MEV)$$

CS-25592

Fig. 64.

THERMONUCLEAR ROCKET

BASIC COMPONENTS

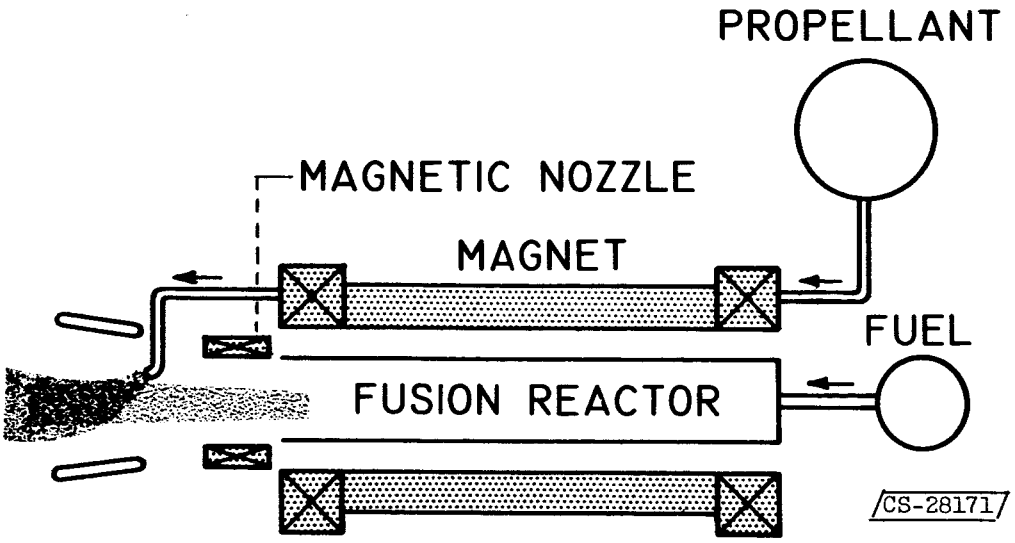

Fig. 65.

THERMONUCLEAR ROCKET

INCORPORATION OF SHIELDED AND CRYOGENICALLY COOLED MAGNET

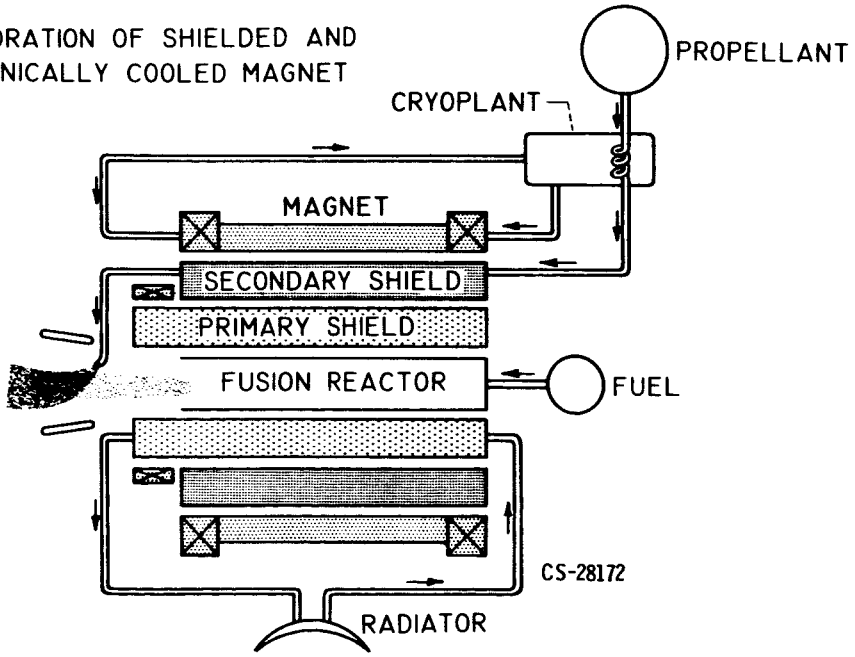

Fig. 66.

THE SOLAR SAIL

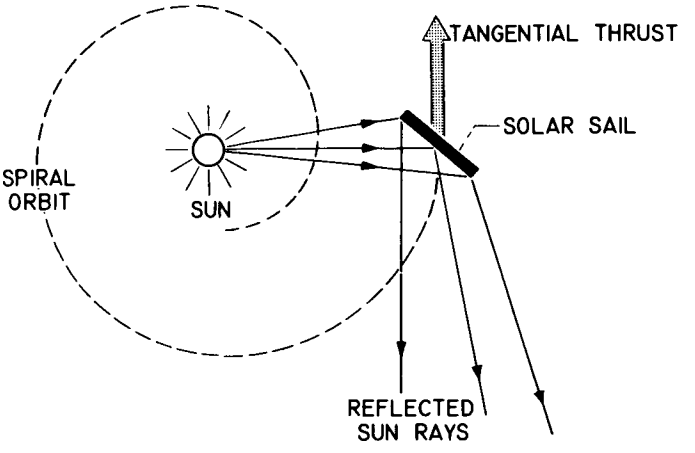

POSITION	MAX THRUST	TANGENTIAL THRUST	TANGENTIAL THRUST TO WEIGHT RATIO
EARTH	1.96×10^{-7} LB/SQ FT	$.755 \times 10^{-7}$	$2. \times 10^{-5}$
VENUS	3.79×10^{-7}	1.46×10^{-7}	3.86×10^{-5}
MERCURY	12.9×10^{-7}	4.97×10^{-7}	13.5×10^{-5}

Fig. 67. CS-18338

THE SOLAR SAIL IN EARTH ORBIT

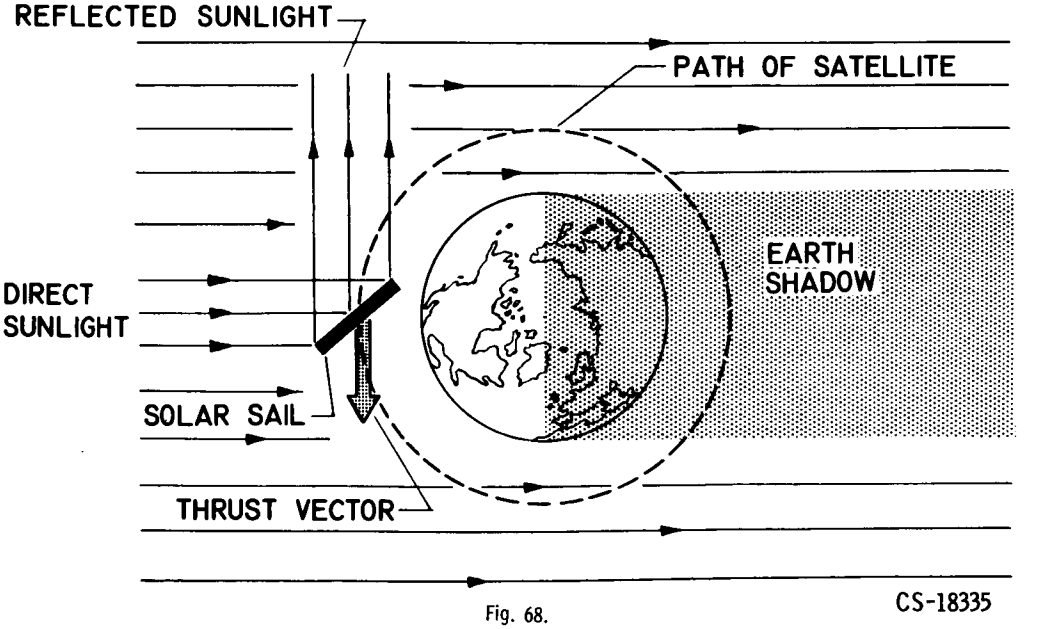

Fig. 68. CS-18335

RADIOISOTOPE SAIL

THRUST/SQ FT	1×10^{-6}
WEIGHT/SQ FT (t = 0.0012")	9×10^{-3}
THRUST/WEIGHT (IDEAL)	1×10^{-4}

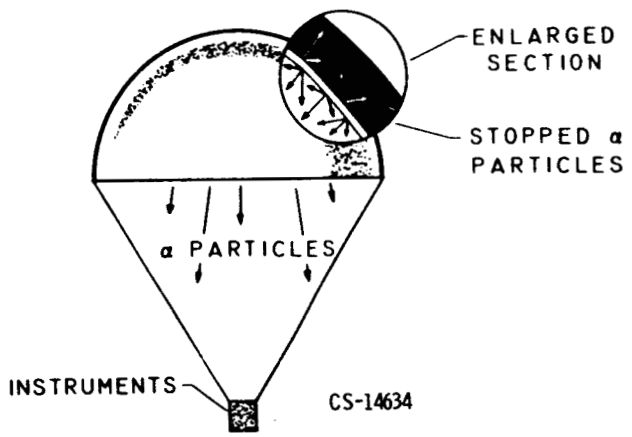

Fig. 69.